ELSEVIER

Physics of the Earth and Planetary Interiors 130 (2002) 209–233

PHYSICS OF THE EARTH AND PLANETARY INTERIORS

www.elsevier.com/locate/pepi

Sources of anomalous transient electric signals (ATESs) in the ULF band in the Lamia region (central Greece): electrochemical mechanisms for their generation

V.-N. Pham [a,*], D. Boyer [a], G. Chouliaras [b], A. Savvaidis [c], G. Stavrakakis [b], J.-L. Le Mouël [a]

[a] *Département de Géomagnétisme (UMR7577, CNRS), Institut de Physique du Globe de Paris, 4 Place Jussieu, 75252 Paris Cedex 05, France*
[b] *Institute of Geodynamics, National Observatory of Athens, P.O. Box 200, 48 Thissio, 11810 Athens, Greece*
[c] *Department of Geophysics, School of Geology, Aristotele University of Thessaloniki, 540 06 Thessaloniki, Macedonia, Greece*

Received 21 November 2001; accepted 14 February 2002

Abstract

Anomalous transient electric signals (ATESs) in the ultra low frequency (ULF) band have been often observed during magnetotelluric (MT) investigations [Nature 319 (1986) 310; Phys. Earth Planet. Int. 114 (1999) 141; Geophys. J. Int. 142 (2000) 948], but their origin was unknown until now. They have the same characteristics as the so-called seismic electric signals (SES) claimed to be earthquake precursors by the VAN group (e.g. [Tectonophysics 110 (1984) 73] and later works by this group). Our analysis suggests that the so-called SES could be of anthropic origin. Following the devastating 7 September 1999 Athens earthquake, the VAN group claimed that a SES had been recorded at LAM station (Lamia, central Greece) some days prior to the main shock and that a second SES, which might correspond to an impending even larger earthquake, had been observed after the main shock. In the 2 years after the Athens main shock, no subsequent large earthquakes have occurred near Athens. We conducted a campaign of measurement in the Lamia region in May and June 2001. The results show that ATESs, which look like SES, have several different sources: pump-stations for ground-water, high power electric lines, and factories located to the SE of Lamia city. The ATESs can be generated by two electrochemical mechanisms of metallic electrode polarization: the "galvanic cell" and the "ac electrolytic cell" which are studied by simulated field experiments and discussed in detail in Appendix A. These two mechanisms can occur over a wide range of length scales in the field. Any isolation failure in buried metallic conductors, such as electrical and telecommunication networks, oil, water and gas pipes, railways, high power electric lines, factories and so on, can produce a galvanic cell or an ac electrolytic cell, or both, which could generate, under some circumstances, an "overvoltage", the ATES. Finally, the absence of a magnetic signal has been observed during ATES and does not constitute a firm criterion for SES [Acta Geophys. Pol. 44 (1996b) 301]. Thus, great care must be taken when claiming the existence of electric precursors of seismic or volcanic events.

Keywords: Seismic electric signals; VAN method; Electromagnetic noise; Electrochemical mechanisms; Anomalous transient electric signals

1. Introduction

Anomalous transient electric signals (ATESs) in the ULF band have been often observed during magnetotelluric (MT) investigation in France, Canada,

* Corresponding author. Tel.: +33-144-272411; fax: +33-144-273373.
E-mail address: vnpham@ipgp.jussieu.fr (V.-N. Pham).

0031-9201/02/$ – see front matter
PII: S0031-9201(02)00008-0

China, Vietnam and Greece (Pham et al., 1986, 1999, 2000). They are distinct from the normal telluric field (natural electric field) in that they do not correlate with the natural magnetic field, so they considerably affect MT results (Pham et al., 1999). It has been difficult to eliminate such noise because of the ignorance of its origin. Since, the initial publications by the VAN group (e.g. Varotsos and Alexopoulos, 1984) claiming the existence of so-called Seismic electric signals (SES) there have been several controversial debates on the VAN method (e.g. Geller, 1996). To resolve this controversy it appears necessary to better understand the origin of SES which, as discussed below, have the same characteristics as ATESs.

We conducted a first campaign of study of electromagnetic noise in the Ioannina region (NW Greece) in June 1997. This region is considered by the VAN group to be the most "sensitive area". This study showed the existence of numerous ATESs at several stations, especially at the station PER installed inside a military base (Pham et al., 1999). It was concluded that the ATESs observed at PER station could have been generated by digital radio-telecommunication transmitters of the military base. However, the ATESs observed at the other sites were recorded only at a single-station and it was not possible to identify their sources.

Following the 7 September 1999 earthquake which severely damaged Athens, a new prediction by the VAN group, based on SES record at the Lamia station (central Greece), aroused new strong controversy via the news media in Greece. On 7 September 1999 at 11:38 GMT an earthquake sequence began 18 km north of Athens with a magnitude $M_L = 3.2$ event, followed by two others smaller shocks at 11:40 and 11:43 GMT both with $M_L = 2.5$. The main shock of the sequence, which occurred a few minutes later at 11:56 GMT with magnitude $M_L = 5.4$, devastated the city of Athens, causing extensive damage to buildings

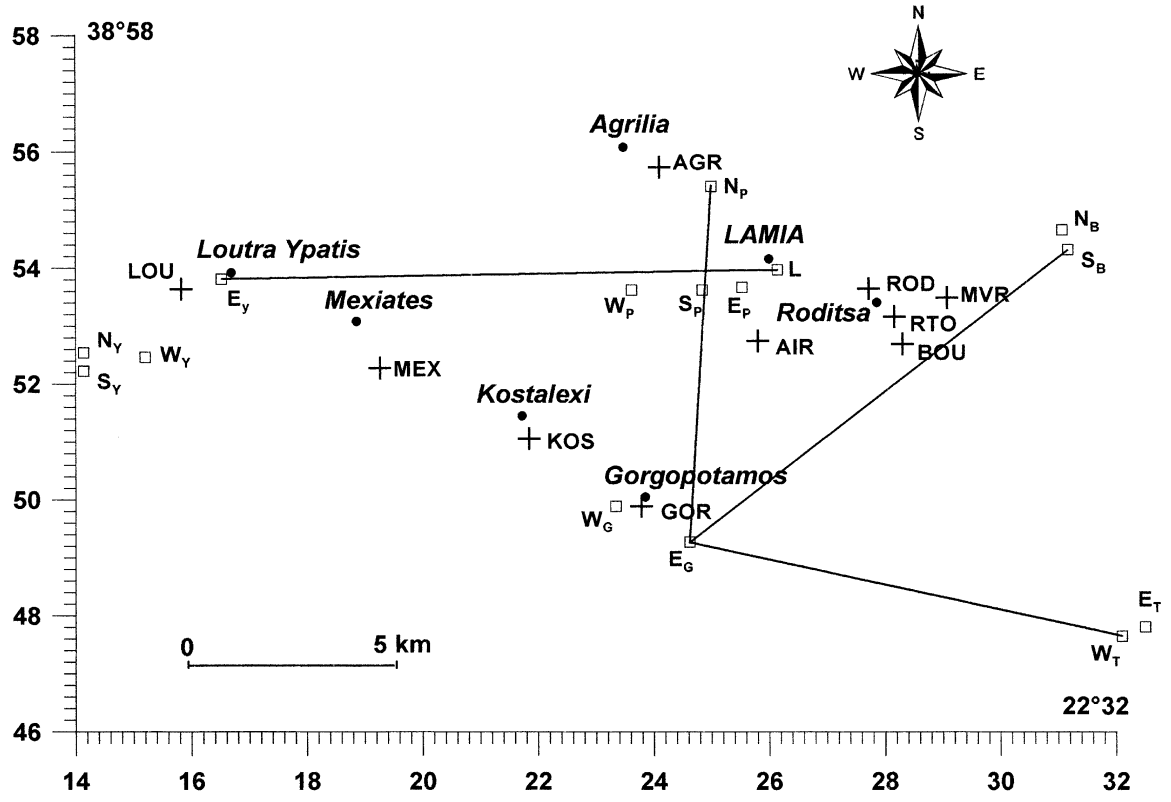

Fig. 1. Location of the sites of measurement (+) of electromagnetic (EM) signals in ULF band in the Lamia region: black circles, centre of Lamia city and surrounding villages; white squares, electric probes of the LAM station of VANs network; thick lines represent some long dipoles, the electric signals of which are shown in Fig. 2.

in the northern and western parts of the city, with a human toll of roughly 100,000 homeless and 143 deaths. The most heavily damaged area was located in the northwestern suburbs of the city; in total 100 buildings collapsed and 13,000 were considered beyond repair.

Immediately after the event, the Geodynamic Institute of the National Observatory of Athens installed an array of 40 portable digital and analog stations in the vicinity of the main shock in order to monitor the aftershock activity. The spatial distribution of epicenters as determined by Stavrakakis et al. (1999) shows a WNW-ESE trend in the epicentral distribution, which is in good agreement with the fault plane solutions determined by Papadopoulos et al. (2000) and Tselentis and Zahradnik (2000), and also with geologic and seismotectonic field investigations by Pavlides et al. (1999, 2000) which indicate that the seismogenic structure consists of a normal fault striking 110–130°N and dipping 50–80°SW.

The moment tensor solution for the main shock, as determined by the USGS, indicates a fault azimuth of 123°, a dip of 55°, a seismic moment of 7.8×10^{24} dyn cm with $M_W = 5.9$, while the Harvard CMT solution gives approximately similar results, with an azimuth of 114°, a dip of 47° and a seismic moment of 1.15×10^{25} dyn cm with $M_B = 5.8$.

One day after the main shock, the VAN group claimed, in a short note submitted to the scientific journal *Acta Geophysica Polonica*, that they had seen anomalous variations of the earth's electric field at their LAM (Lamia, central Greece) measuring site some days prior to the main shock (on 1 and 2 September). According to their observations and interpretation, the observed variation was composed of

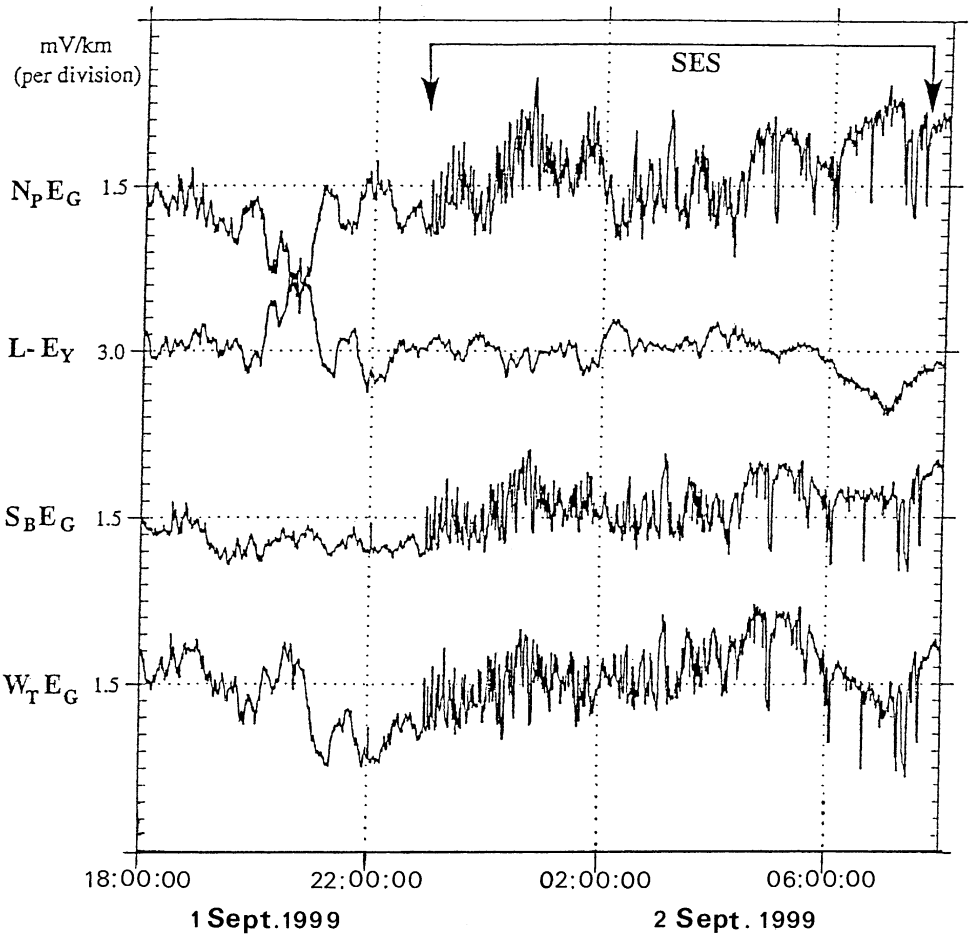

Fig. 2. Examples of the so-called SES recorded at LAM station (as shown in Fig. 1) on 1 and 2 September 1999 and interpreted as precursors of the 7 September 1999 Athens earthquake by the VAN group (redrawn from Varotsos et al., 1999a).

two anomalous signals in time (the so-called SES). They hypothesized that if the first SES activity was associated with the Athens main shock, then the second SES signal might correspond to a hypothetical second larger earthquake: "... the second might correspond to an impending comparable (or slightly larger) EQ. ... the strongest earthquake usually occurs during the 4th week or 2 weeks later" (Varotsos et al., 1999a).

A few days later, on 13 September the VAN group submitted another short note to *Acta Geophysica Polonica* stating that they had recorded new SESs at LAM on 12 and 13 September and claiming that this strengthened their original interpretation regarding an impending second larger main shock with an epicenter "... a few tens of kilometer..." away from the Athens epicentral area, possibly at the Atalanti fault which lies between Lamia and Athens (Varotsos et. al., 1999b,c).

Even though the above information and a prediction of a second large earthquake after the Athens event was confidentially communicated by the VAN group to the Ministry of Public Works (responsible for evaluating predictions), this information leaked to the Greek mass media and a relevant article also appeared abroad as early as 24 September in the news columns of the journal *Science* (Vol. 285 (5436), p. 2044). More than 2 months after the Athens earthquake, on 18 November 1999 at the meeting of the Seismological Society of Japan in Sendai, Japan, a paper entitled "recent developments in the VAN method" by Varotsos and Uyeda, maintained the same prediction.

In the 2 years after the September 1999 Athens main shock, no large earthquakes occurred in or near Athens. Thus, research should be conducted to better understand the physical mechanism of the generation of VANs signals in order to be able to correctly evaluate these data in a scientifically rigorous manner. It is, therefore, necessary to study the characteristics of the electromagnetic signals in and near Lamia city, where the LAM station of the VAN network was installed.

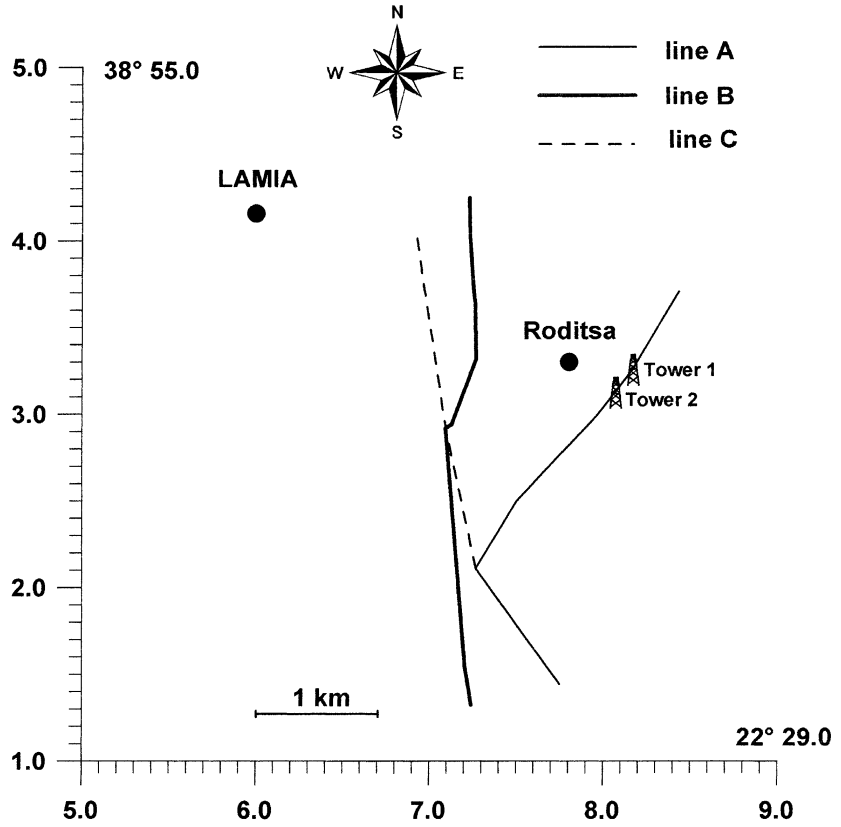

Fig. 3. Location of the centre of Roditsa village (black circle) to the SE of the Lamia city and of three high power electric lines. EM signals were recorded near the towers 1 and 2 on the line A (as shown in Fig. 9).

2. Lamia campaign of measurement

The objective of our study is to determine whether or not anomalous transient electric signals (ATESs) exist in the ULF band and, if they exist, to identify their origin. In May and June 2001, we conducted a campaign of electromagnetic measurements in the Lamia region. Our data acquisition system, described in a previous paper (Pham et al., 1999), is a high sensitivity MT instrument designed for MT surveys. It is composed of five channels covering a broad band of frequencies (10^{-3}–10^{3} Hz).

The electromagnetic signals can be recorded in different ranges of frequencies upon request. During the Lamia campaign, most signals were recorded in two ranges of the ULF band (0.01–1 and 0.001–0.1 Hz).

The LAM station of the VAN network is composed of several long (>10 km) and short electric dipoles; the location of VANs electric probes is indicated by white squares in Fig. 1. Thick lines correspond to long dipoles. VANs anomalous transient electric signals (labeled SES in Fig. 2) were recorded on 1 and 2 September 1999 and claimed by the VAN group as associated with the 7 September 1999 Athens earthquake (Varotsos et al., 1999a). Note that SES were observed only on the long dipoles located to the SE of Lamia city (N_PE_G, S_BE_G, W_TE_G) and not on the long dipole located to the west ($L–E_y$). Therefore, the SE region was considered by Varotsos et al. (1999a) as an "SES sensitive area" of the Lamia site.

According to the VAN group (Varotsos et al., 1993), there are three types of SES: single SES, SES activity, and gradual variation of electric field (GVEF). A single SES is a signal isolated in time having a duration ranging from half-a-minute to several hours, whereas, in SES activity a number of SES appear within a short-time, such as a few hours or a day. GVEF have a duration of many hours to days. Another characteristic

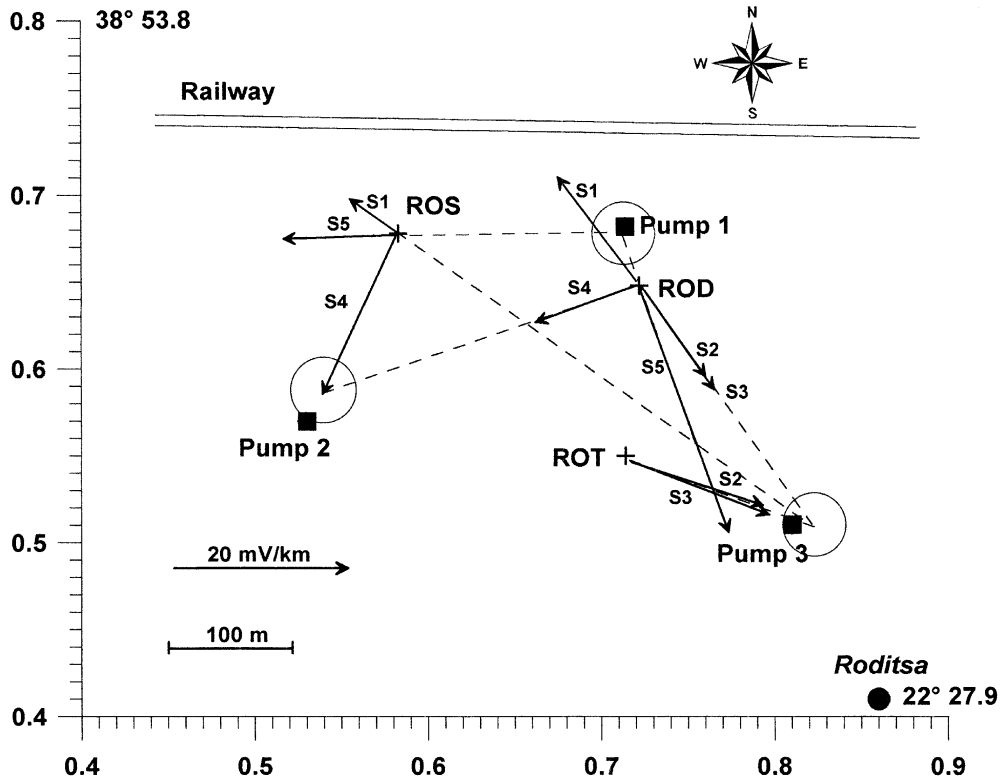

Fig. 4. Results of a detailed study in the northern part of the Roditsa village with two double-stations ROD–ROT and ROD–ROS: arrows represent the amplitude and the direction of the ATESs; a pair of arrows of the same signal number corresponds to signals recorded simultaneously at the double-station; five typical pairs of arrows (S1–S5) are shown; dashed lines are their prolongation until intersection area (white circles); black squares, pumps located above drill-holes.

claimed for SES is the absence of magnetic signals correlated with the electric signals (Varotsos et al., 1996b). The signals recorded on 1 and 2 September 1999 at LAM station (as shown in Fig. 2) were considered as typical SES activity by the VAN group (Varotsos et al., 1999a).

The ATESs closely resemble the single SES or SES activity which is frequently reported by the VAN group as the basis for their short-term earthquake predictions (Varotsos et al., 1996a). In order to detect ATESs, we installed and operated several stations around Lamia city (+ signs in Fig. 1). Using four channels of our instrument, we recorded two components of the electric field and two components of the magnetic field along two perpendicular directions, 15 and 105°N which correspond to the structural directions of the Lamia graben. The electric dipoles along 15 and 105°N were 50–100 m long, and are referred hereafter, respectively, as NS and EW. The horizontal magnetic components in these two same directions are, respectively, referred to as H and D.

After 1 day of recording at each station, no significant ATESs were observed to the west of Lamia city, but that their number increased to the east. Finally, the most "active area" was localized near the Roditsa village to the SE of Lamia city (as shown in Figs. 1 and 3).

3. Detailed study near the Roditsa village: methodology for detection of the ATESs sources

Roditsa is a village located about 3 km SE of Lamia city where three high power electric lines intersect (as shown in Fig. 3). In the northern part of the village there is a large olive grove where it is possible to install several monitoring stations in order to localize the sources of ATESs. This methodology, which was first successfully used in France (Pham et al., 2001),

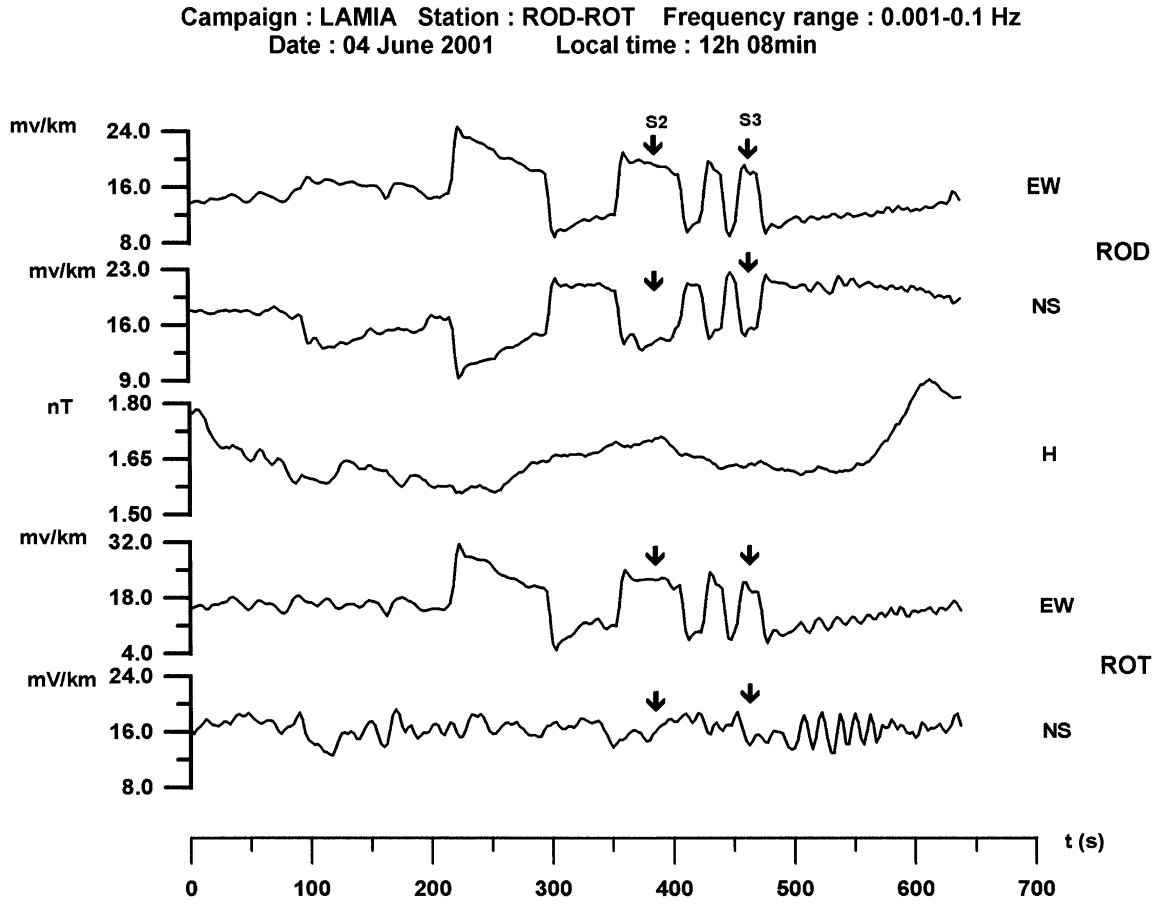

Fig. 5. Example of ATESs recorded at the double-station ROD–ROT. S2 and S3 are the signals numbers shown in the Fig. 4.

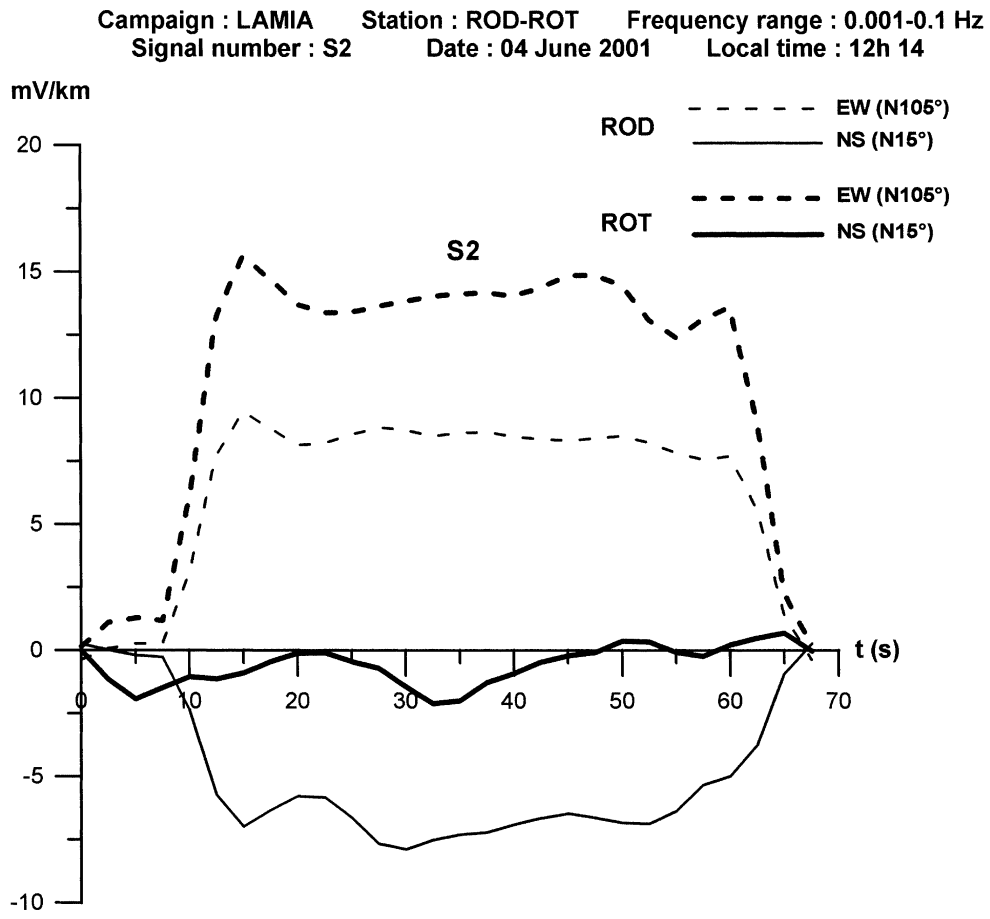

Fig. 6. Example of isolated signal S2 extracted from Fig. 5.

consists of simultaneous measurement of the electric field at two stations called hereafter a "double-station". At each station measuring two orthogonal electric components allows us to determine the amplitude and the direction of the electric field vector. As indicated previously, the two electric components were measured at two stations, respectively, along N15 and N105°, referred in the figures as NS and EW.

Fig. 4 shows the location of two double-stations, ROD–ROS and ROD–ROT. Our five channel instrument allows us to record simultaneously four electric components (e.g. two at ROD and two at ROT) and only one H near ROD station. Fig. 5 shows an example of the signals recorded at ROD–ROT. We can observe clearly the existence of a train of ATESs simultaneously at ROD and ROT stations without any correlation with the H. Each ATES was isolated in order to determine the amplitude and the direction of the electric field. Fig. 6 shows an example of the isolated signal S2, and Fig. 7 shows the polarization diagram of the electric field at these two stations. Fig. 8 shows another example of ATESs recorded at the double-station ROD–ROS; the polarization and the amplitude of the signal S1 were determined by the same procedure. From the intersection of the direction of the two electric vectors at each double-station, we can localize the potential source of the ATES. In the field, the geographical co-ordinates of each station were measured by a portable GPS with a precision about 10 m. The precision of the direction of the electric field depends on the amplitude of the ATES and the background noise. The mean error was estimated to be about $\pm 3^\circ$ which corresponds to a deviation of ± 5 m at a distance of 100 m from the station. Taking all the factors in account, we estimate the mean deviation of the intersection point of the

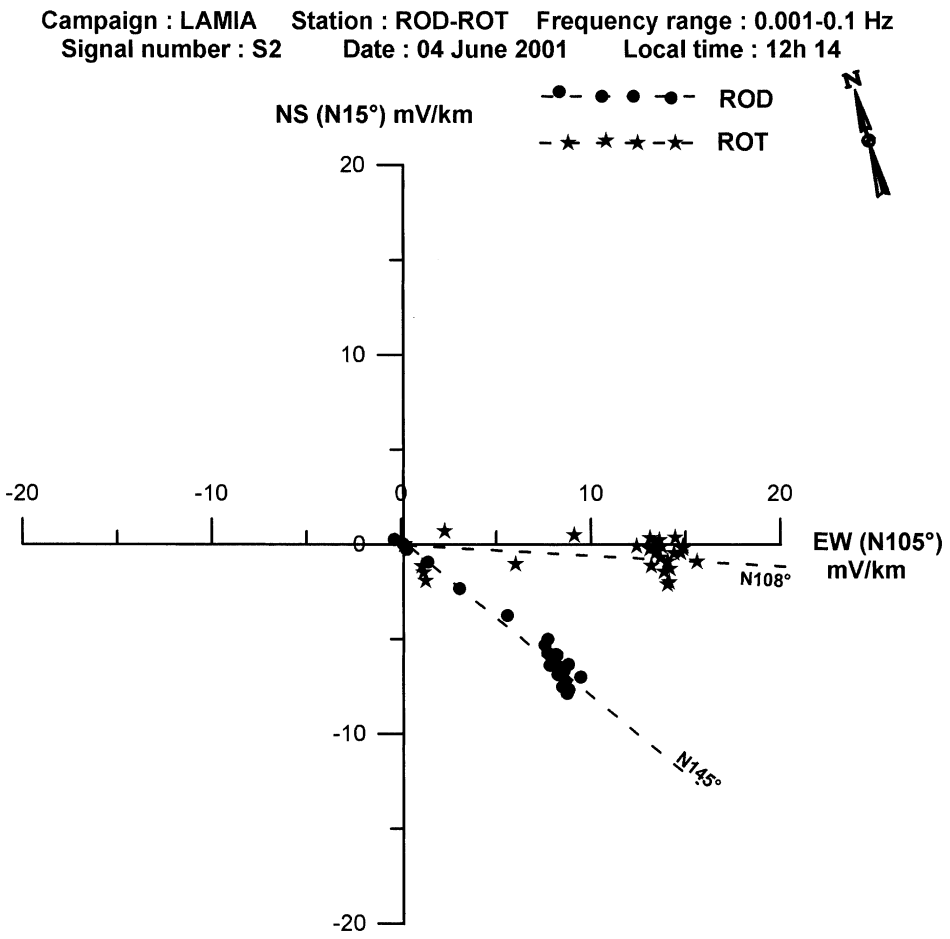

Fig. 7. Example of polarization diagram obtained from the isolated signal S2, showing two polarization directions obtained by least-squares fit and corresponding respectively to stations ROD and ROT.

two electric vectors to be about 50 m. This is represented by a circle of 50 m of diameter in Fig. 4. Obviously, this deviation increases with the distance of the intersection point from the double-station. Our last work in the field was to look for the presence of a possible source inside the deviation circle area. By using two double-stations ROD–ROS and ROD–ROT, we have localized three intersection zones represented by three circles in the Fig. 4. In the field, we discovered the existence of three pumps for ground-water, Pumps 1–3, near these three intersection points.

Around Roditsa village there are many ground-water drill-holes for domestic use, agriculture and olive groves. All drill-holes are tubed by metallic pipes reaching the aquifer nappe at a depth of 40–60 m. Some drill-holes are connected with permanent pumps and the others with mobile pumps. Leakage of water along a metallic pipe can generate ATESs by electrochemical mechanisms, as discussed below in Appendix A.

4. ATESs generated by high power electric lines

As shown in Fig. 3, Roditsa village is surrounded by three high power electric lines. In fact, the electromagnetic noise at high frequencies (>10 Hz) is very important in the studied area. Our objective is to determine whether high power electric lines can generate ATESs in the ULF band. We have carried out one double-station RTO–RTW near two towers, towers 1 and 2, located to the SE of Roditsa village on the path of power line A (as shown in Figs. 3 and 9).

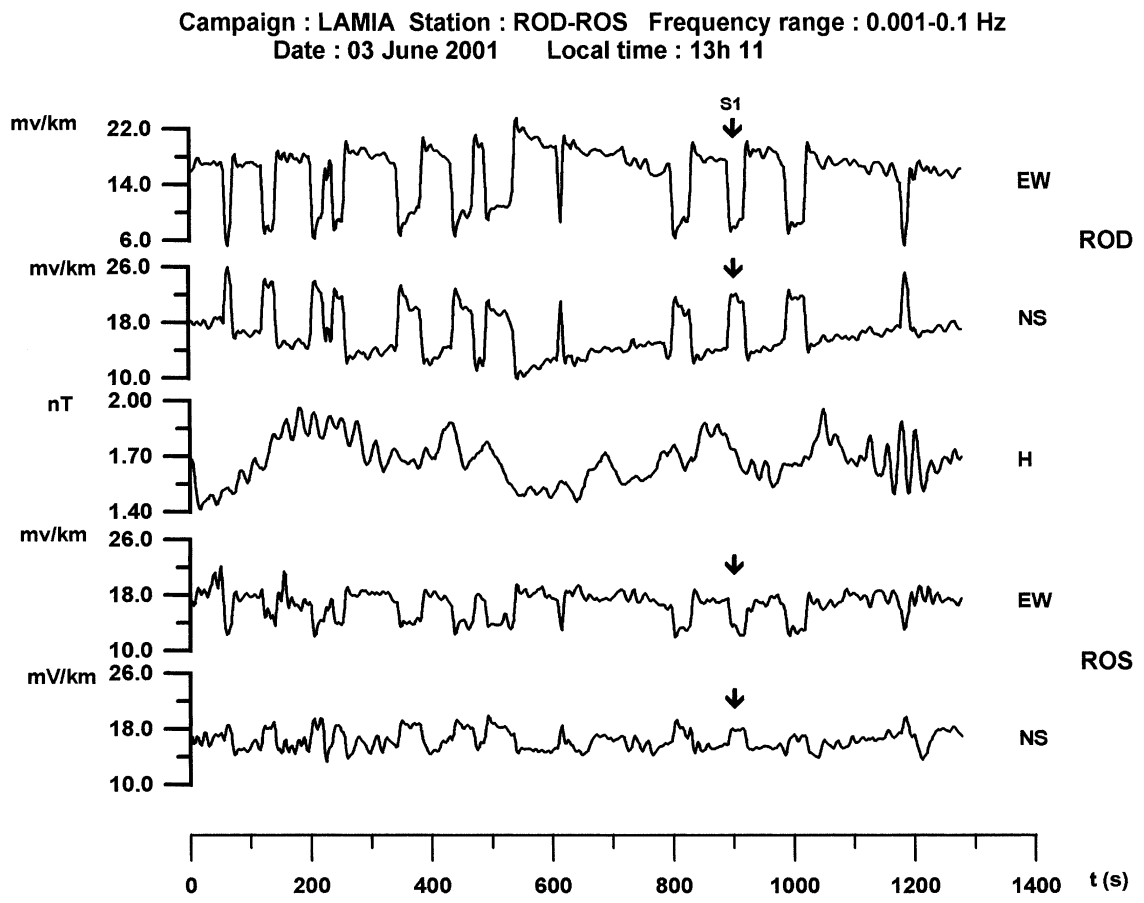

Fig. 8. Example of ATESs recorded at the double-station ROD–ROS. Signal S1 is shown in the Fig. 4.

Fig. 10 shows an example of the signals recorded at this double-station, confirming clearly the existence of several ATESs of different durations (10–100 s) and of different amplitudes. We have selected one typical transient signal R1 to study its polarity, as shown in Fig. 9. It is interesting to observe that the intersection point is localized near tower 1. Other signals in Fig. 10 have the same characteristics. Again, these signals have the same characteristics as the so-called SES, without any correlation with the H. This observation is important for the discussion below about the origin of SES.

5. ATESs generated by factories

Around Roditsa village there are also many factories which can generate electromagnetic noises, but their characteristics are not well known. We have carried out a four channels single-station (BOU in Fig. 1), located about 150 m from the Bourougani factory which specializes in metallic construction (Fig. 11). Here, the electromagnetic noise generated by the factory is very important, as mentioned below. During the recording of the four electromagnetic components (EW, NS, H and D) in the frequency range of 0.01–1 Hz, the activity of the factory stopped for half an hour for lunch. In Fig. 12, between 12:00 and 12:30 local time, the noise disappears completely on the two electric components EW and NS and has little influence on the two magnetic components H and D. This explains why no anomalous transient magnetic signal was observed in low frequency ranges (<0.1 Hz) in correlation with ATES, as shown by the signal B5 in Fig. 13. In this range, the natural magnetic field (the MT field) is much larger than the artificial magnetic field, which cannot be observed on the record. Therefore, the absence of a magnetic signal in the ULF band does not constitute a

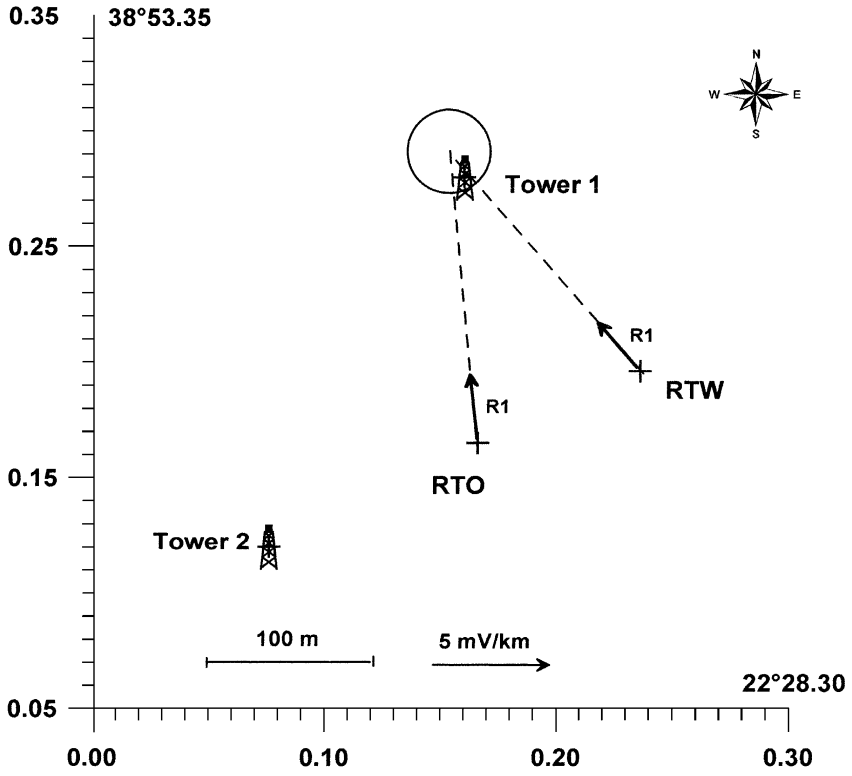

Fig. 9. Location of the double-station RTO–RTW near the towers 1 and 2 on the high power electric line A (as shown in Fig. 3).

firm criterion to discriminate the so-called SES from artificial signals, contrary to VANs assertion (Varotsos et al., 1996b). In higher frequency ranges, short and strong transient signals appear clearly on all electric and magnetic components (Fig. 14). The polarization vector of several ATESs are shown in Fig. 11; thick arrows correspond to long duration signals (~50 s) and dashed arrows to short duration (~5 s). The polarization of all arrows points in the direction of the factory.

6. Electrochemical mechanisms for the generation of dc signals: possible sources for ATESs

The results presented above for the Lamia region, indisputably confirm the artificial origin of ATESs and probably of SES which have the same characteristics. Prior to this study, their sources were unknown and their origin could not be satisfactorily explained. Recently, ATESs have been observed at the "Centre de Recherche Géophysique (CRG)", Garchy located in the center of France and their origin has been clearly identified with the leakage of electric and phone networks of the CRG (Pham et al., 2001). They can be explained by two electrochemical mechanisms of the metallic electrode polarization: the "galvanic cell" and the "ac electrolytic cell" which are described in detail in Appendix A. Let us briefly recall here the phenomenon of electrode polarization. Exploration geophysicists have long known that an electric potential difference exists between two metallic electrodes driven into the soil. When a metallic electrode is in contact with an electrolyte, metal ions pass into the solution and an equilibrium is reached, characterized by an electric potential difference (EPD) between the metal and the electrolyte. If the electrode is electrically isolated, the metal ions are firmly attached to the interface by electrical or chemical forces, or both, forming a "double electric layer", also called a "Helmholtz layer" (Bard and Faulkner, 1980; Besson, 1984); an EPD results between the metallic electrode and the electrolyte contained in the soil, and can be computed theoretically by the Nernst equation (as shown in

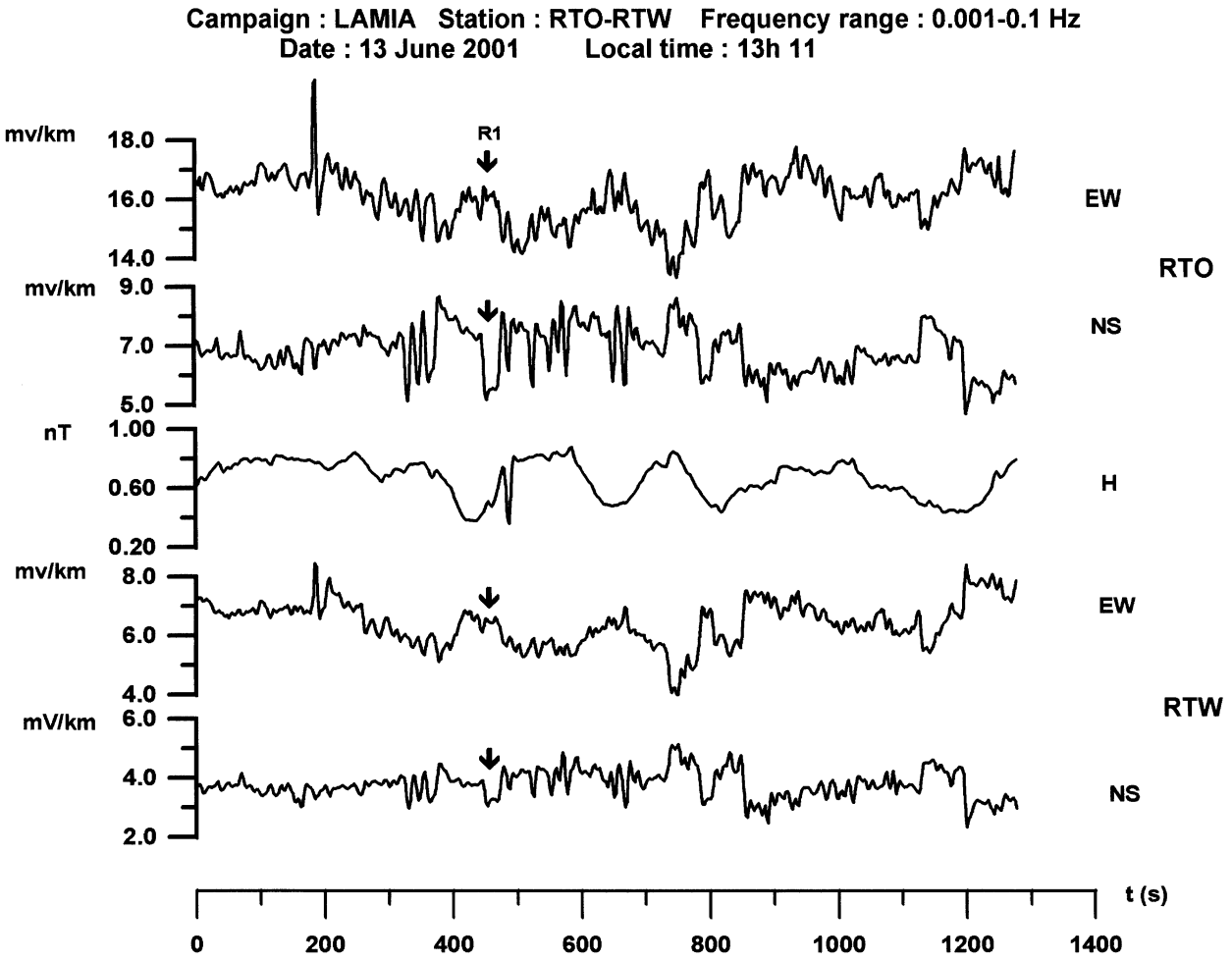

Fig. 10. Example of ATESs recorded at the double-station RTO–RTW. Signal R1 is shown in the Fig. 9 with the intersection area (white circle) close to tower 1.

Appendix A). When two metallic electrodes are connected externally by a conductor, a spontaneous electrochemical reaction occurs: this constitutes a "galvanic cell" which works like a battery and converts chemical energy into electrical energy. A galvanic cell, like a battery connected to the soil by two electrodes, can generate a dc potential at the ground surface. A variation of the electrochemical reaction produces a variation of dc potential and consequently generates an electric field around the electrodes, the "transient electric signal". Another type of electrochemical generator exists when two metallic electrodes are connected with an external dc voltage, constituting an "electrolytic cell" (Bard and Faulkner, 1980; Besson, 1984). Recently we have demonstrated that two metallic electrodes connected with an ac external voltage can also constitute an electrochemical generator and generate a transient electric signal in the ULF band (as shown in Appendix A).

Let us now examine different types of ATESs sources identified in the Lamia region. The first type was localized under the ground-water pumps, which are connected to metallic pipes driven into the drill-holes. The leakage of the water (galvanic cell), or the leakage of the electric current of the pumps (ac electrolytic cell) along the metallic pipe constitutes a dc generator. The variation of the voltage (the "overvoltage") of this generator, generates a transient electric signal, the ATES.

The second type of ATESs source is high power electric lines. Contrary to expected results, ATESs in the ULF band cannot be generated by the electric

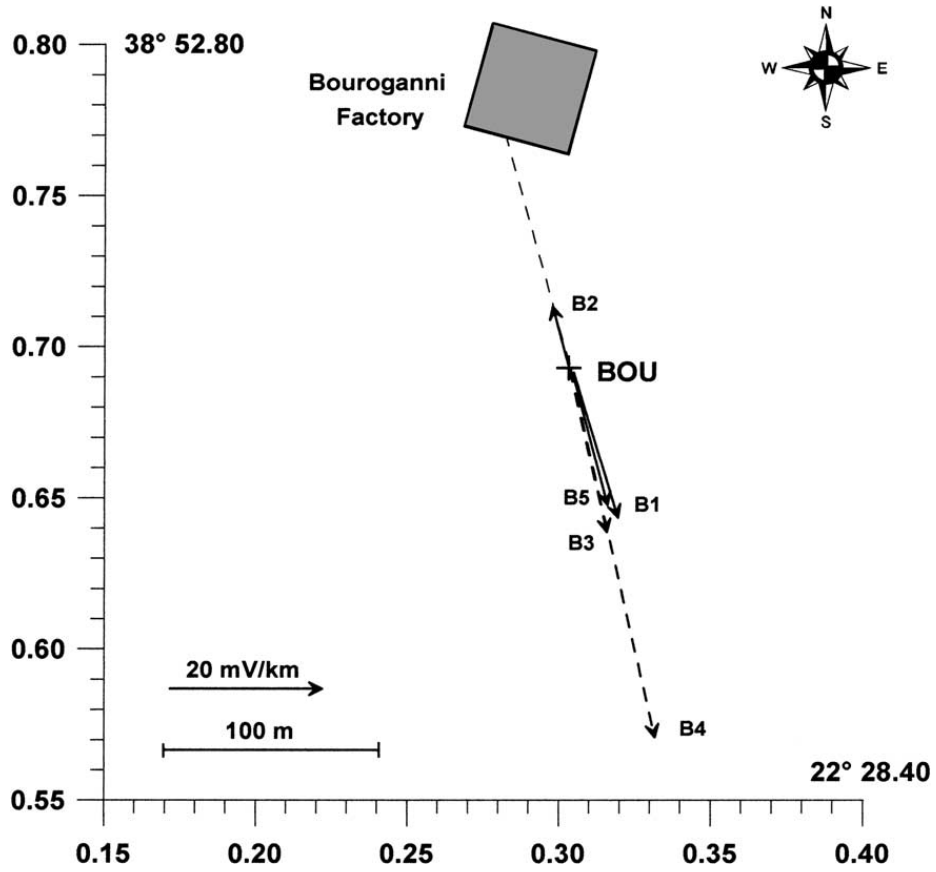

Fig. 11. Location of the single-station BOU (see Fig. 1) near the Bouroganni factory: thick arrows, polarization of some ATESs in low frequencies range (0.001–0.1 Hz); dashed arrows, polarization of some ATESs in higher frequencies range (0.01–1 Hz).

lines themselves, considering their characteristic form and their very low frequency range. The results shown in the Figs. 8 and 9 can more probably be explained by the leakage of the ground cable under tower 1. Finally, the ATESs observed near the Bouroganni factory have the same origin, i.e. the leakage of the electrical network of the factory into the ground during its activity.

7. Discussion and conclusion

With the new methodology of measurement by a double-station undertaken in the Lamia region, the sources of ATESs can be now identified and their origin explained by electrochemical mechanisms. It appears now possible that most ATESs observed in the Ioannina region (Pham et al., 1999) have the same origin. As in the case of the Lamia basin, there are many drill-holes for ground-water in the Ioannina basin, many high power electric lines and factories along the valley.

It is, to our knowledge, the first time that the existence of dc signals generated by two different mechanisms has been clearly demonstrated by simulated (Appendix A), local (Garchy) and regional (Lamia) field experiments. These results can be generalized at different scales and for different field conditions. Any isolation failure in buried metallic conductors such as electrical and telecommunication networks, water and gas pipes, railways and so on, can, in some circumstances, produce a galvanic cell able to generate significant currents if such isolation failure is connected to the soil. On the other hand, any leakage in the ac distribution network, for domestic or industrial use, high power electric lines, electric

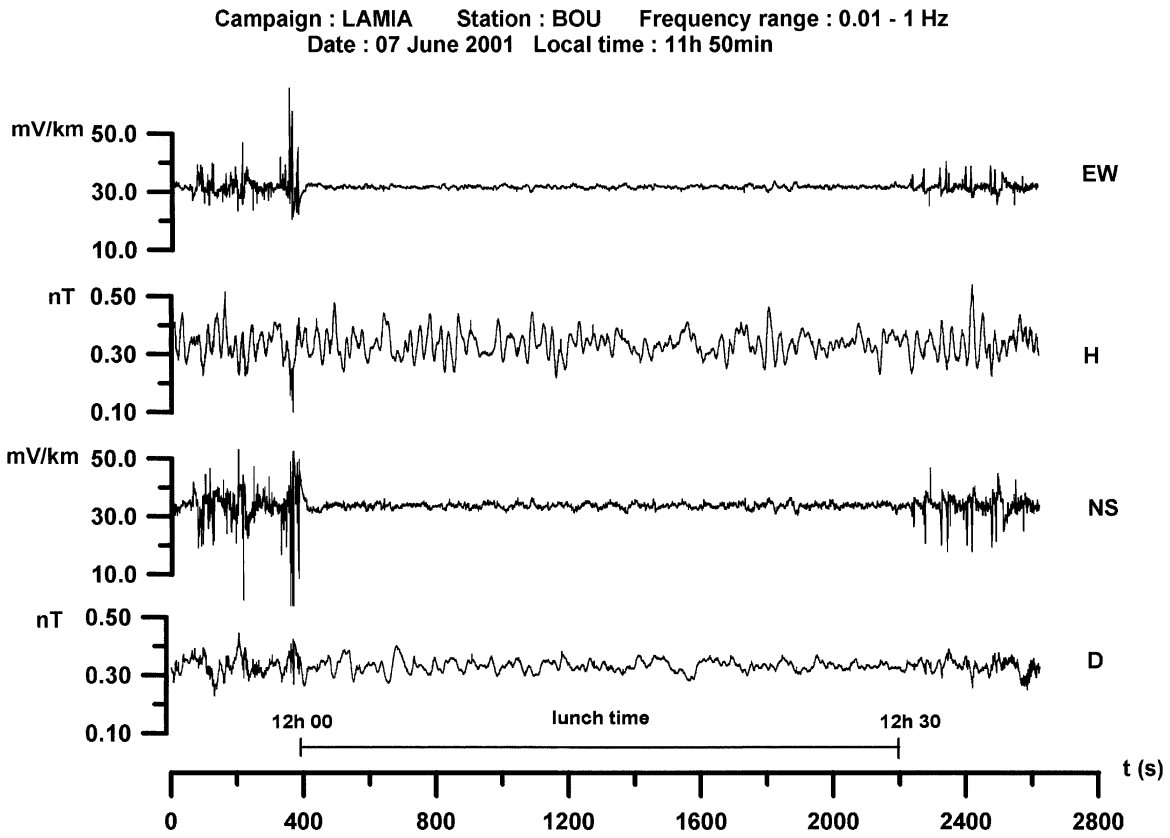

Fig. 12. EM signals recorded at the BOU station during lunch time.

railway power sub-stations, etc. can constitute an ac electrolytic cell. These situations are frequently encountered in developed countries and sites near such facilities are definitely not appropriate for monitoring hypothetical "natural" electric signals possibly associated with seismic activity. It is very surprising that some electrical probes of VAN stations are installed inside big cities as Ioannina and Lamia, and that some of their long dipoles (>10 km) are connected with electric and phone lines around these same cities. Indeed, long dipoles integrate, not only different kinds of noise covering large regions but also large electrical discontinuities in the ground which make it impossible to identify correctly the sources of any anomalous signals.

Finally, we have demonstrated that the absence of a magnetic signal during ATES can occur from anthropic causes and, therefore, need not be a "firm criterion" for SES.

We conclude that the greatest care must be taken in claiming the existence of electrical precursors (the so-called SES) of seismic significance. First, it is necessary to choose monitoring sites far away from any noise sources, such as the different types of noise sources described in this paper. In addition, the design of the monitoring instrument must allow us to localize the anomalous electric sources through the use of sets of multiple stations. Only if the signals do not correspond to any artificial potential source might it be possible to argue for a natural origin. Until now, none of the so-called SES published in different papers (e.g. Varotsos et al., 1999a; Uyeda et al., 2000) satisfies these criteria. The failure of the prediction of the VAN group after the 7 September 1999 Athen's earthquake appears to have been due to considering the noise at LAM station as an SES. This should serve to make researchers who work on possible electromagnetic effects associated with earthquakes and volcanoes, more cautious in their interpretation of the origin of anomalous electromagnetic signals in any range of frequencies.

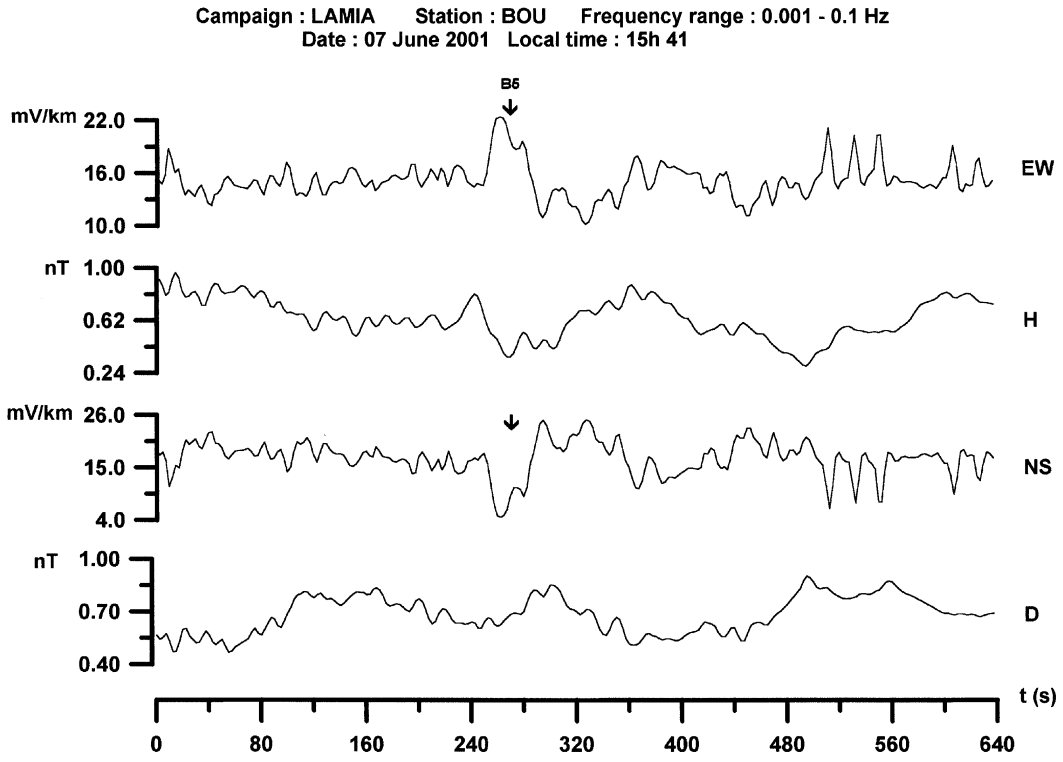

Fig. 13. Example of long ATESs recorded at BOU station in the frequencies ranges of 0.001–0.1 Hz. Signal B5 is shown in the Fig. 11.

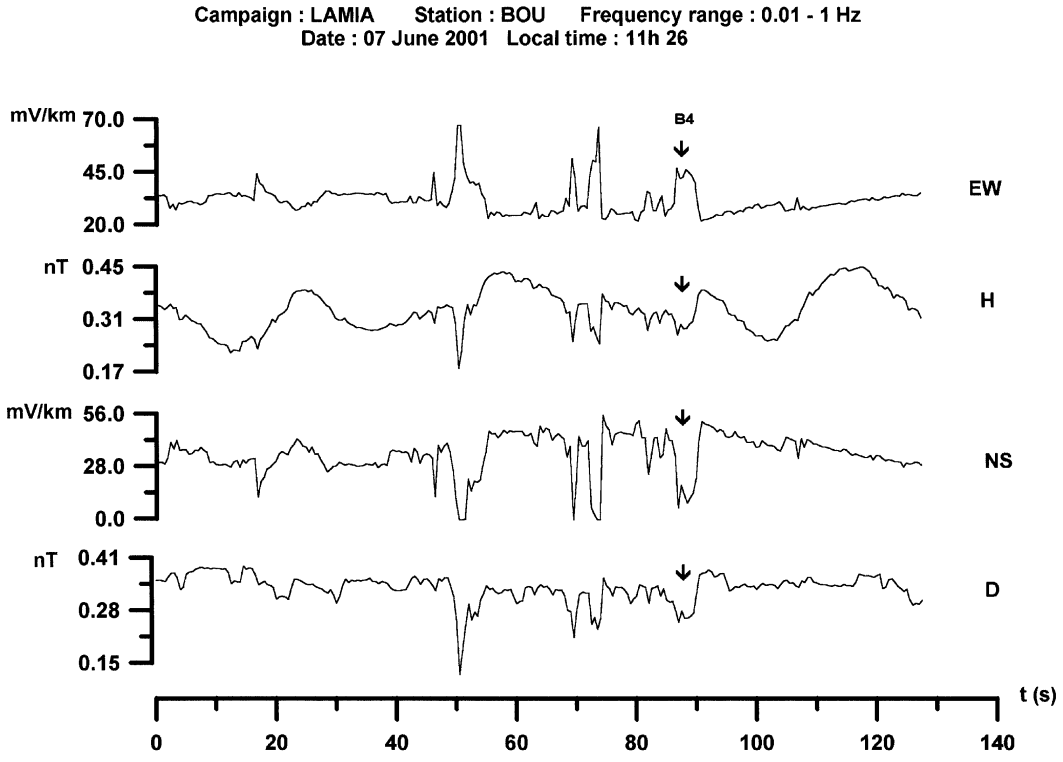

Fig. 14. Example of short and strong ATESs recorded at BOU station in frequencies ranges of 0.01–1 Hz. Signal B4 is shown in the Fig. 11.

Acknowledgements

The field work in Lamia region was supported by the Greek Ministry of Public Works within the project "Electromagnetic Investigations in the Boarder Area of Atalanti, Central Greece". We are grateful to A. Tsekouras for his help in the field. The theoretical and experimental studies of the electrochemical mechanisms were realized within the French Space Agency detection of electro-magnetic emissions transmitted from earthquakes regions program (DEMETER). We are indebted to R.J. Geller for his careful reading and correction of our manuscript.

Appendix A. Electrochemical mechanisms for generation of dc signal associated with metallic electrode polarization

A.1. Nernst equation, normal and standard potentials of an electrode

When a metallic electrode (M) is in contact with an electrolyte containing the same ions M^+ as the metal, the metal/electrolyte couple then constitutes a definite (M/M^{n+}) redox pair, where n is the valence of the metal ion. Thermodynamic principles can then be used to compute the absolute potential of the electrode $V_{\text{abs.elect.}}$ as a function of the metal ion concentration. This is the Nernst equation (Bard and Faulkner, 1980; Besson, 1984):

$$V_{\text{abs. elect.}} = V_0 + \left(\frac{RT}{nF}\right) \ln(a_{M^{n+}}) \quad \text{(A.1)}$$

R is gas constant $= 8.37 \times 10^7$ cgs; F, Faraday constant = 96,500 C; T, absolute temperature; $a_{M^{n+}}$, activity of the ions M^{n+}, V_0, "normal potential" of the metal.

Note that neither $V_{\text{abs.elect.}}$ nor V_0 can be measured in absolute value. Only relative values can be measured with respect to another electrode, referred to as a "reference electrode". In electrochemistry, the standard hydrogen electrode (SHE) is chosen as reference electrode and for a temperature of 25 °C and pH = 0, the voltage of the SHE is taken as 0 V. It is then possible to measure the electric potential difference (EPD) between a metal electrode and the SHE and a scale of the "standard potentials" $V_{\text{st.}}$ of the redox pairs of the various metals can be obtained. Values of some standard potentials are given in Table A.1 at 25 °C (Besson, 1984), the standard potential of the H_2/H^+ redox pair being zero by convention.

Table A.1
Selected standard potential $V_{\text{st.}}$ at 25 °C for some metal/ion couples (from Besson, 1984)

Metal/ion couple	Standard potential $V_{\text{st.}}$ (mV)
Ag/Ag^+	+800
Cu/Cu^{2+}	+340
H_2/H^+	0
Pb/Pb^{2+}	−130
Fe/Fe^{2+}	−440

This scale gives a quantitative measurement of the strength of the redox pairs. Larger standard potentials correspond to higher oxidizing power, and smaller (and negative) standard potentials correspond to higher reducing power. It also allows us to calculate the relative potential V_r of an electrode with respect to a reference electrode:

$$V_r = V_{\text{abs. elect.}} - V_{\text{abs. ref.}} = V_{\text{st. elect.}} - V_{\text{st. ref.}} \quad \text{(A.2)}$$

In the field conditions, the SHE reference electrode can be replaced by a non-polarizable electrode such as a $Pb/PbCl_2$ electrode. The relative potentials were measured for 12 cylindrical metallic electrodes driven into the soil. As the relative potentials V_r depend on the surface contact area s between the electrodes and the soil, one has $V_{rs} = V_r/s$ (expressed in mV/dm^2) the relative specific potentials which are given in Table A.2 and ordered according to the nature of the electrodes.

The relative specific potentials V_{rs} of Table A.2 cannot be directly compared with the standard potentials of Table 1 as they depend on the in situ conditions. Nevertheless, for electrodes of the same nature, values of V_{rs} of the same order are found. Stainless steel and copper have V_{rs} values larger than iron or raw steel. In addition, the hierarchy of voltages between copper and iron, for example is conserved between Tables 1 and 2. Therefore, it seems reasonable, as a first approximation, to apply the classical rules of electrochemistry to the experimental results obtained in the field in order to understand the effect of electrode polarization in geophysical systems.

Table A.2
Specific potential of some types of metallic electrodes, relative to a non-polarizable electrode ($Pb/PbCl_2$) and measured in the field

Electrode number	Nature	Diameter (cm)	Contact surface (dm^2)	Relative specific potential V_{rs} (mV/dm^2)
A_1	Stainless steel	1	1.10	+585
A_2	Stainless steel	1	1.10	+604
A_3	Copper	2	2.21	+229
A_4	Copper	2	2.21	+210
A_9	Copper	2	2.21	+221
A_{10}	Copper	2	2.21	+213
A_5	Iron	1	1.10	+134
A_6	Iron	1.6	1.93	+17
A_7	Iron	1.5	1.65	+62
A_8	Iron	2.3	2.53	+36
A_{11}	Raw steel	1.4	2.14	−5
A_{12}	Raw steel	1.4	2.14	+8

A.2. Electrochemical generators and the Butler–Volmer equation

Recall that an "electrochemical cell" (or "electrochemical generator") is a pair of metallic electrodes separated by one or several electrolytes. A cell is referred to as "polar" if the electrodes are of different nature (Rochaix, 1996). From the values of V_{rs} given in Table 2 polar cells have an EPD stronger than non-polar cells. By contrast, if the EPD is zero, the cell is referred to as "non-polarized". It is the case for electrodes called "non-polarizable", an improper term as, in fact, these electrodes are designed to have the same relative potential, and their EPD is small and close to zero (a few mV), depending on their quality. Such electrodes were used as reference electrode in our experiments in order to eliminate the large and time dependent contact electric potential of metallic electrodes.

If two metallic electrodes are joined by an external conductor (for example, a copper wire or a resistance), current flows in a definite direction. This system, referred to as a "galvanic cell" then works as a battery. Conversely, by using an external current generator, one can impose a definite electrical current between the electrodes. Such a cell is called an "electrolytic cell". This case has been studied extensively by electrochemists with dc current generators. In both cases, there is "polarization" if the electrodes are modified by the current flow.

What is needed here from chemical kinetics is a relationship between the electric current density i in the two electrodes and the variation of their relative potential or voltage, referred to as "overvoltage" η. For each electrode, one can determine the curve $i = f(\eta)$ called "polarization curve". This curve is characteristic of the redox couple associated to each electrode and can be described theoretically by the Butler–Volmer equation (Bard and Faulkner, 1980; Besson, 1984). For a redox couple M/M^{n+}, the reaction is represented by the equation:

$$M \underset{\text{reduction}}{\overset{\text{oxidation}}{\rightleftarrows}} M^{n+} + ne^- \tag{A.3}$$

and the Bultler–Volmer equation can be written as (Rochaix, 1996):

$$i = i_0(e^{\alpha A\eta} - e^{-\beta A\eta}) \tag{A.4}$$

where $A = nF/RT$ is constants defined in Eq. (A.1); i_0, exchange current density; α, anodic transfer coefficient for reaction (A.3) in the direction of oxidation; β, cathodic transfer coefficient for reaction (A.3) in the direction of reduction with $\alpha + \beta = 1$.

The first term in Eq. (A.4) represents the anodic component of the current density while the second term represents the cathodic component.

Examples of theoretical polarization curves described by the Butler–Volmer relation are shown in Fig. A1 for various values of the exchange current density i_0 (Bard and Faulkner, 1980). The current

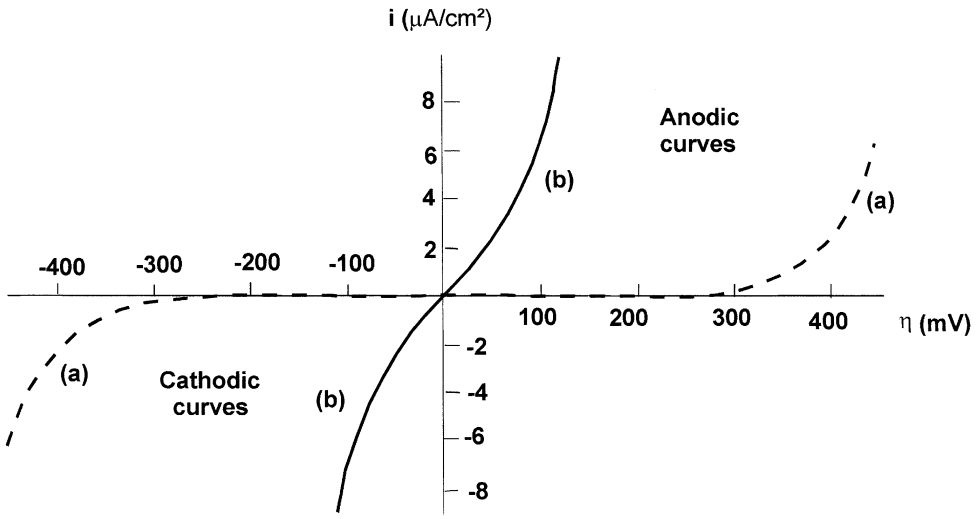

Fig. A1. Theoretical symmetric polarization curves ($\alpha = \beta = 0.5$), according to the Butler–Volmer relation, for two exchange current density i_0: (a) $i_0 = 10^{-9}$ A/cm^2; (b) $i_0 = 10^{-6}$ A/cm^2 (redrawn from Bard and Faulkner, 1980).

density i_0 depends on the electrolyte composition and on the contact between the electrode and the electrolyte. For small values of i_0, the reaction at the electrode is slow and the slope di/dη at the origin is small (case (a) in Fig. A1). Conversely, for large values of i_0, the reaction is fast and the slope at the origin is large (case (b) in Fig. A1). The part of the curve relative to positive overvoltage is the "anodic curve" which corresponds to oxidation in the redox couple (Eq. (A.3)). The part of the curve relative to negative overvoltage is the "cathodic curve" which corresponds to reduction in Eq. (A.3).

By convention, the electrode where oxidation takes place is called "anode" and corresponds to the negative pole of the electrochemical generator. The electrode where reduction takes place is called "cathode" and corresponds to the positive pole (Rochaix, 1996). Indeed, electrons of the anode are transferred by the external circuit (as shown in Fig. A2), thus, reducing the number of the negative charges of its Helmholtz capacitor, allowing the ions M^{n+} to move away from the anode and produce oxidation of the metal. Conversely, electrons reaching the cathode through the external circuit attract ions M^{n+}, which cannot move away from the interface and undergo reduction.

The theoretical polarization curve in Fig. A1 is symmetrical with respect to the origin, corresponding to the case $\alpha = \beta$ in Eq. (A.4): the reaction kinetics is the same for oxidation and reduction. In practice,

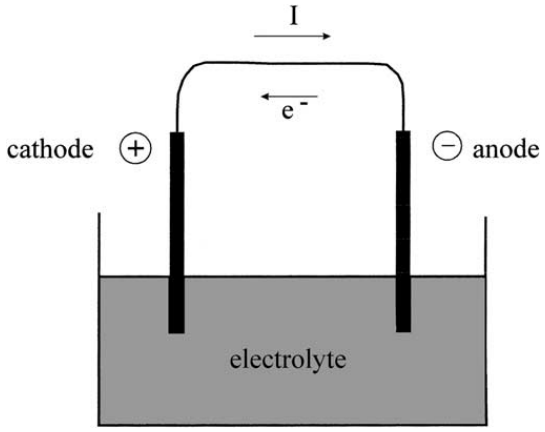

Fig. A2. Definition of "anode" and "cathode" in an electrochemical cell.

the two reactions do not have the same kinetics, anodic and cathodic curves differ and the polarization curve becomes asymmetrical. This asymmetry is well confirmed by following field experiments at the Fontainebleau site located at about 60 km south of Paris. The soil consists of very thick and homogeneous sandstone.

A.3. Determination of polarization curves for a galvanic cell in the field

A galvanic cell is an electrochemical generator made of two metallic electrodes connected by a

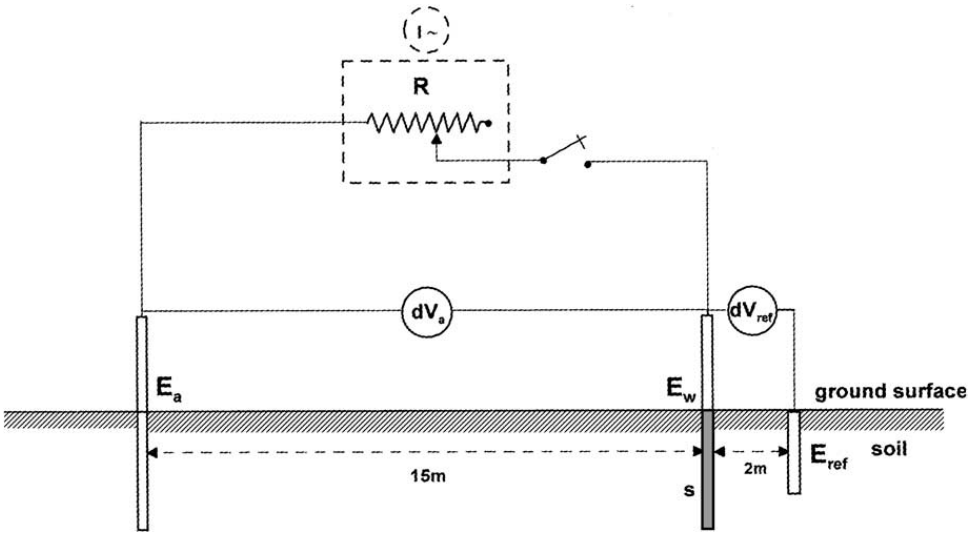

Fig. A3. Electrodes set-up in the field for plotting of the polarization curves: E_w, metallic working electrode; E_a, metallic auxiliary electrode; $E_{ref.}$, non-polarizable reference electrode; s, surface contact of working electrode with the soil; R, potentiometer for "galvanic injection"; $I\sim$, ac current generator for "50 Hz injection".

conductor (of resistance R). The set-up for determination of the polarization curves in the field (Fontainebleau site) is displayed in Fig. A3. The studied electrode is referred to as the working electrode E_w. Current flows is obtained when the electrode E_w is connected to the auxiliary electrode E_a through a variable resistor R (with a maximum resistance (R_{max}) of 10 kΩ) and a switch. The potential difference dV_a measured between E_w and E_a when the switch is closed ("galvanic injection"), gives the intensity of the current $I_a = dV_a/R$. If s is the electrode surface area in contact with the soil, the injected current density is $i = I_a/s$. Here the reference electrode $E_{ref.}$ is a non-polarizable electrode. If $(dV_{ref.})_1$ is the potential difference measured between E_w and $E_{ref.}$ before the injection (open circuit), and $(dV_{ref.})_2$ is the measured potential difference during the injection, then the overvoltage is $\eta = (dV_{ref.})_2 - (dV_{ref.})_1$. The polarization curve is obtained by varying the value of the resistance R.

The results are shown in Fig. A4 for three groups of electrodes: iron electrodes (A_6, A_7 and A_8), raw steel electrode (A_{12}), and copper electrodes (A_3, A_4 and A_9). For iron and raw steel electrodes, the auxiliary electrode is a copper electrode (A_{10}). Indeed, from Table 2, it can be observed that iron and raw steel working electrodes have relative specific potentials smaller than the copper auxiliary electrode. Hence, E_w corresponds to the negative pole of the generator, the anode, which induces oxidation in the working electrode with a positive overvoltage. This is confirmed by the measurements displayed in Fig. A4. Conversely, when the working electrode is a copper electrode, and taking in this case an iron electrode (A_5) as the auxiliary electrode, cathodic curves are observed, with negative values of the overvoltage η. In this galvanic system, iron and raw steel electrodes are oxidized while the copper electrodes are reduced by the current flow.

The most interesting result of Fig. A4, however, is the clear asymmetry between anodic curves (iron and raw steel groups) and the cathodic curves (copper group). The slope at the origin of anodic curves is systematically larger than the slope at the origin of the cathodic curves: the oxidation of iron is faster than the reduction of copper.

Finally, we observe that the polarization curves are not rigorously the same within a given group. In practice, a non-polar cell made of electrodes of the same nature could, in some cases, constitute an electrochemical generator, with values of the overvoltage smaller than in the case of a polar cell.

The most important result to keep in mind is that any galvanic cell, made of electrodes of the same nature or not, can behave as a generator of dc current as long as the relative potential difference V_r is large

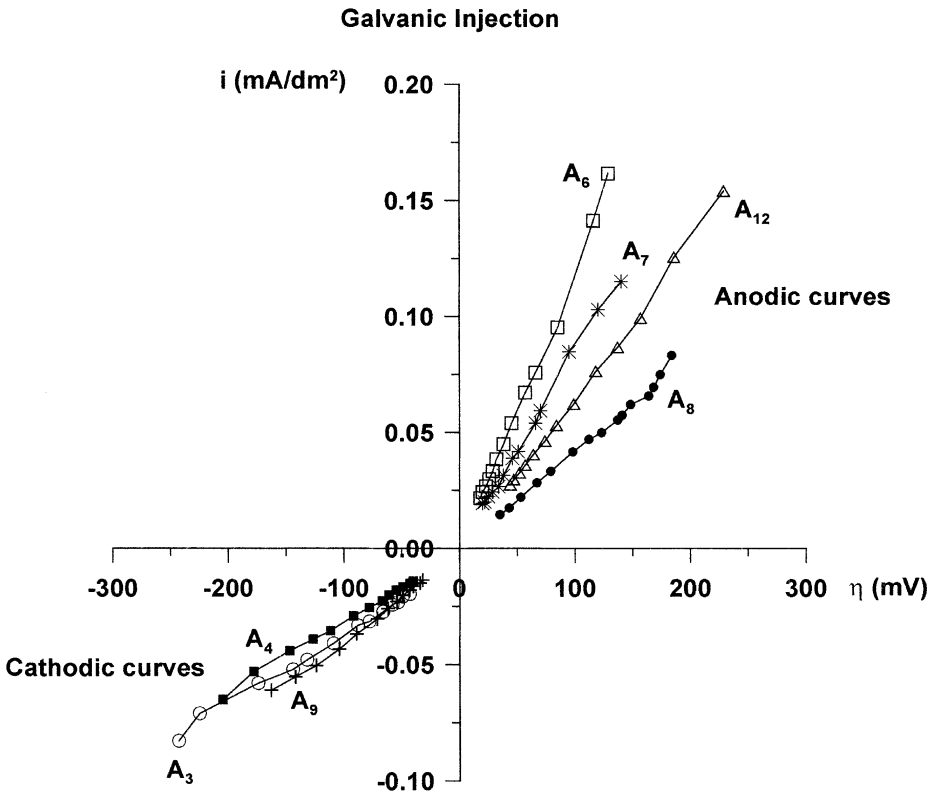

Fig. A4. Galvanic injection polarization curves for different groups of metallic working electrodes: anodic curves (iron group); cathodic curves (copper group).

enough. In addition, when the two electrodes are connected, they do not have the same behaviour, each of them undergoing a specific chemical reaction with its surrounding electrolyte. An electrochemical generator, therefore, does not behave as an ideal dc current generator like a battery.

A.4. Determination of polarization curves for an ac electrolytic cell in the field

Recall that an electrolytic cell is made of an electrochemical cell in which electrical current flow is imposed by an external generator. Usually in electrochemistry dc current generators are used. Here, we shall concentrate rather on an electrolytic cell using an ac current generator, and in particular, we shall study whether some part of the energy is converted into dc current.

For this purpose, the same set-up as before is used (Fig. A3), replacing the resistor R by an ac current generator at a frequency of 50 Hz ("50 Hz injection"). The effective ac current intensity I_{eff} is measured with a meter connected in series with the generator. As before, the ac current density is obtained from the known contact surface area s with the soil as $i_{\mathrm{eff}} = I_{\mathrm{eff}}/s$. The value of the overvoltage η is obtained as before in the case of the galvanic injection. The measured ac current density is then plotted as a function of the overvoltage, defining ac polarization curves $i_{\mathrm{eff}}(\eta)$. Obviously the values of I_{eff} are not algebraic. By convention, I_{eff} is plotted with the same sign as η, for comparison with the case of galvanic injection.

The polarization curves have been determined for the same electrode groups (iron, raw steel, copper), but, in this case, the same copper electrode (A_{10}) was used as auxiliary electrode for all working electrodes, including copper electrodes. By contrast with the galvanic cell for which the value of the non-polar Cu/Cu cell EPD is too small, the effective ac intensity of the current for the electrolytic cell is always large enough to produce measurable values of the overvoltage η. The results are displayed in Fig. A5.

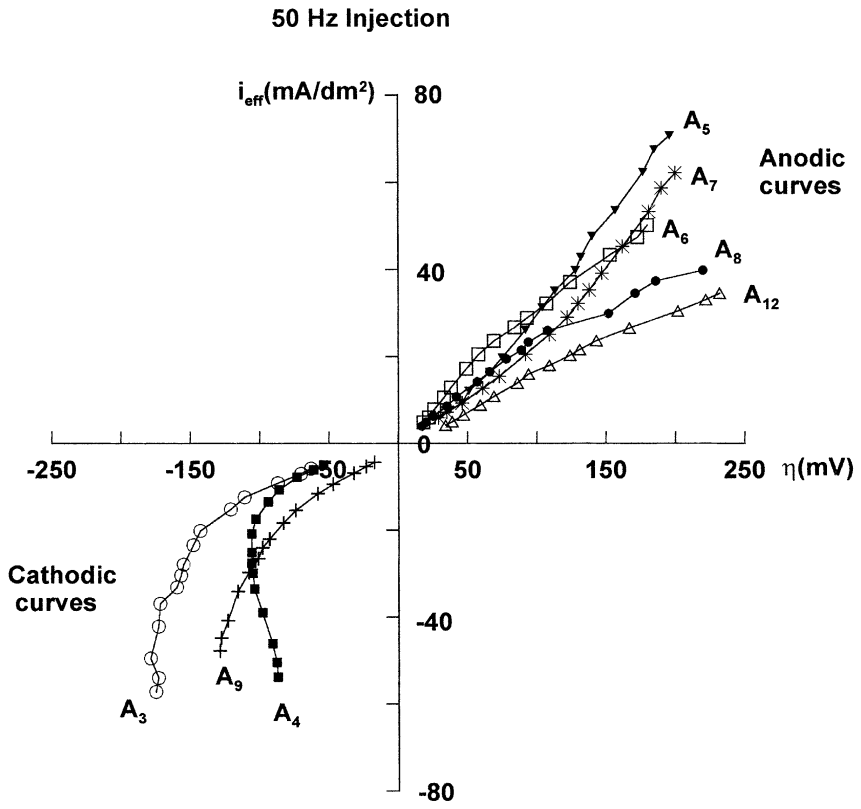

Fig. A5. The 50 Hz injection polarization curves for different groups of metallic working electrodes: anodic curves (iron group); cathodic curves (copper group).

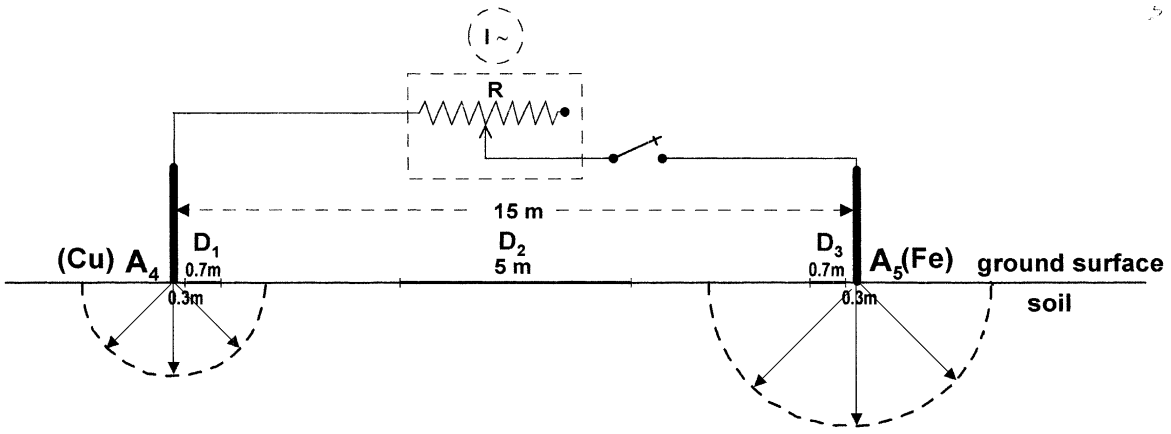

Fig. A6. Field experiment using two metallic electrodes A_4 (Cu) and A_5 (Fe), and three pairs of non-polarizable electrodes (dipoles D_1, D_2 and D_3) for measuring the electric field. During the "galvanic injection", A_4 and A_5 are connected with a potentiometer R ($R_{max} = 10\,K\Omega$). During the "50 Hz injection", A_4 and A_5 are connected with an ac 50 Hz generator providing a variable ac current intensity. Radial arrows symbolize the polar electric field specific to each metallic electrode.

The first conspicuous result is that an ac current at the frequency of 50 Hz through metallic electrodes, of the same or of a different nature, can produce a dc voltage, or, rather a dc overvoltage. In the case of a polar cell (Fe/Cu, raw steel/Cu), the resulting effect is similar to the behaviour observed with the galvanic cell: iron and raw steel electrodes pick up a positive overvoltage and the resulting polarization curves are anodic. Copper electrodes pick up a negative overvoltage, and their polarization curves are cathodic, independent of the sign of the initial relative voltage V_r of the working electrode with respect to the auxiliary electrode. In addition, like in the case of the galvanic polarization curves, an asymmetry is observed between anodic and cathodic curves, but the difference is larger compared with the galvanic injection curves. Moreover, the ac polarization cell appears more general, as the order of magnitude of the overvoltage is similar for any electrode couples, even if they are of the same nature (non-polar cells). The resulting effect of the ac injection is the appearance of a "polarization" at the interface between metal/electrolyte, generating a specific overvoltage for each electrode. This behaviour can be explained by the general tendency of the dc polarization curve to be asymmetric, a character which must remain during the 50 Hz injection. The alternating current, therefore, creates alternatively positive and negative overvoltages of different amplitudes. The electrode, therefore, behaves as a rectifier, producing a dc voltage (Besson, 1984).

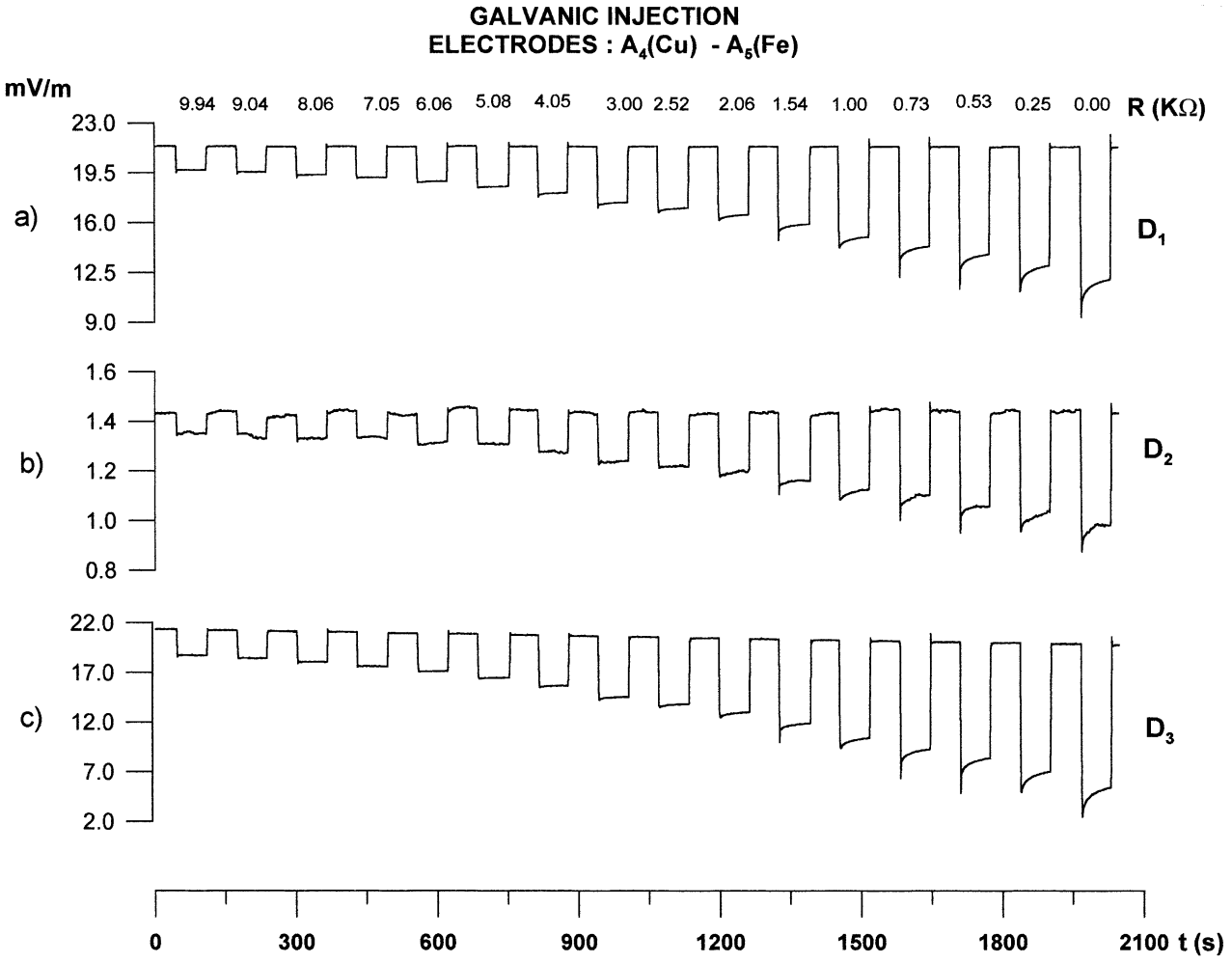

Fig. A7. Records of the electric signals corresponding to the three dipoles during the galvanic injection between A_4 and A_5: (a) dipole D_1; (b) dipole D_2; (c) dipole D_3. The values of the resistance R (in KΩ) corresponding to different injections are indicated at the top of the figure.

A.5. Simulated field experiment for generation of dc signal by electrochemical generators

If two electrodes inserted in a soil (containing an electrolyte) are connected by a conductor (galvanic injection) or an ac current generator, we expect that an electrical current will be produced in the soil: the cell will be equivalent to a dc current generator, transforming chemical energy into electrical energy (or ac electrical energy into dc energy). As in the case of regular dc electrical resistivity survey, a current distribution will be produced in the soil, and its potential can be mapped with non-polarizable electrodes (in order to eliminate spurious static potentials).

This mechanism was checked with a simulated experiment in the field (Fontainebleau site). A polar cell made of two metallic electrodes (one copper electrode A_4 and one iron electrode A_5) was installed in the soil with a distance of 15 m between the electrodes (Fig. A6). These electrodes were connected by the resistor R ($R_{max} = 10\,k\Omega$) and a switch, or the 50 Hz ac generator used before. Three potential differences on the A_4–A_5 line were measured using three dipoles (Fig. A6), giving the electric field in three points: D_1 (length 0.7 m, located 0.65 m away from A_4), D_2 (length 5 m, with its centre located in the middle of the A_4–A_5 line), and D_3 (length 0.7 m, located 0.65 m away from A_5). These three dipoles used non-polarizable electrodes, and were connected to an amplifier and data acquisition system.

The measured electric fields (in units of mV/m) are shown for the three dipoles for galvanic injection obtained by varying the resistance value R (Fig. A7). For each injection, the switch is closed for about 1 min. The signals have a rectangular shape typical of such injections. A priori, if overvoltages effects at the

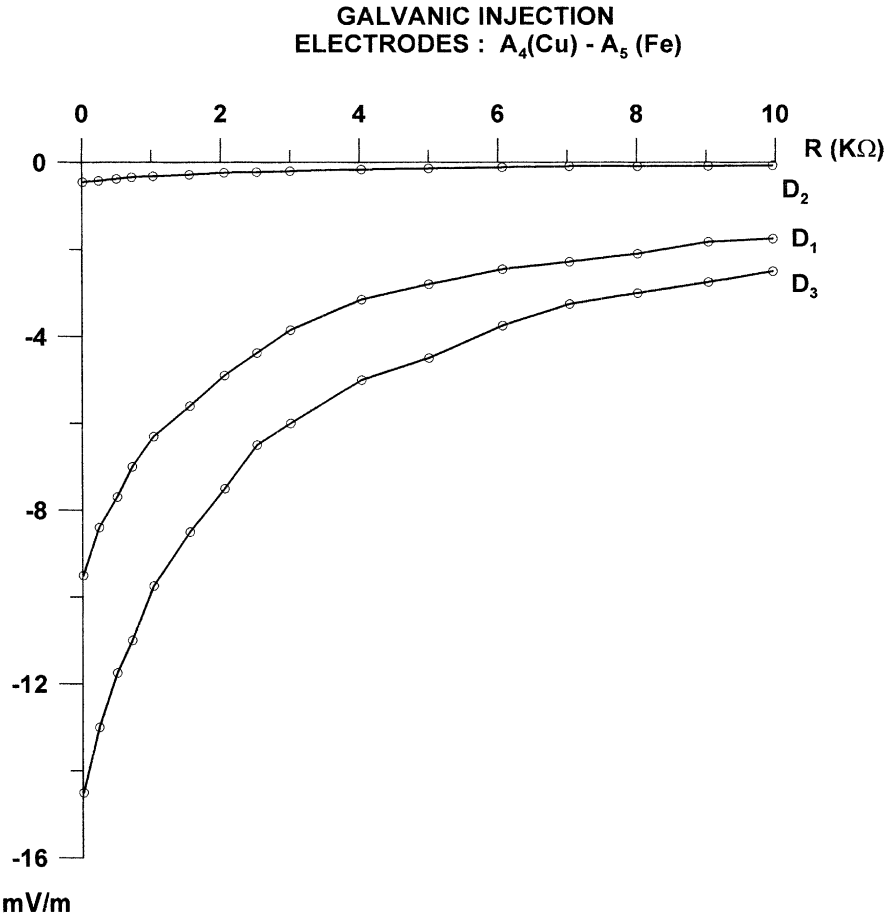

Fig. A8. Galvanic injection between A_4 and A_5. Variation of the amplitudes of the pulse signals vs. the resistance R for the three dipoles D_1, D_2 and D_3.

metal–electrolyte interface are ignored, one would expect that during a galvanic injection, for a homogeneous field resistivity, the electric fields should be equal in D_1 and D_3. This is not observed. The measured pulse signals associated with the various injections are displayed in Fig. A8 for the three dipoles. Compared with dipole D_2, the electric fields measured by dipoles D_1 and D_3 are larger, which is normal because these dipoles are closer to the injection points provided by the electrodes. However, the unexpected result is that the electric fields given by D_1 and D_3 are significantly different. As discussed before, one has to accept the evidence that the electrodes are characterized, during the injection, by an overvoltage resulting in an additional dc current, controlled by the details of the electrochemical reactions happening at the metal–soil interface. Each electrode can be assumed to behave as an individual point source of current, symbolized by radial arrows on the Fig. A6.

For ac 50 Hz injection, the same set-up is used as before, replacing the resistor by an ac current generator (as shown in Fig. A6). The results are displayed in Fig. A9. First of all, we obtain a confirmation that an ac current injected through metallic electrodes can produce significant dc voltage in the soil. Like in the case of the galvanic injection, different amplitudes are obtained for the fields D_1 and D_3 (Fig. A10). In this case, however, a significantly different behaviour is observed with dipole D_1 compared with dipole D_3. Note also that the maximum amplitude obtained in this experiment (60 mV/m) is significantly larger than the maximum amplitude of 15 mV/m observed

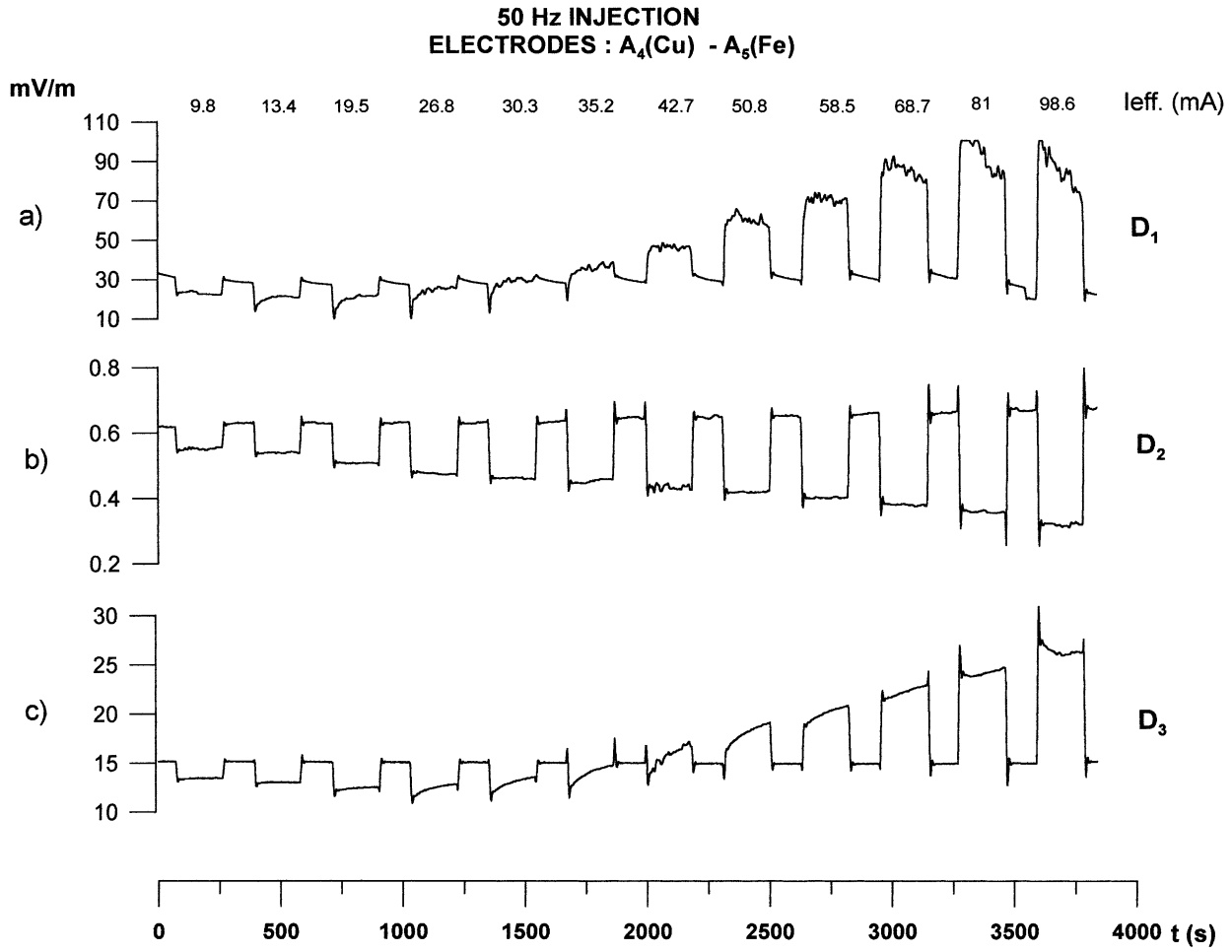

Fig. A9. Records of the electric signals for the three dipoles during the 50 Hz injection between A_4 and A_5: (a) dipole D_1; (b) dipole D_2; (c) dipole D_3. The values of the ac current intensity (in mA), are indicated at the top of the figure.

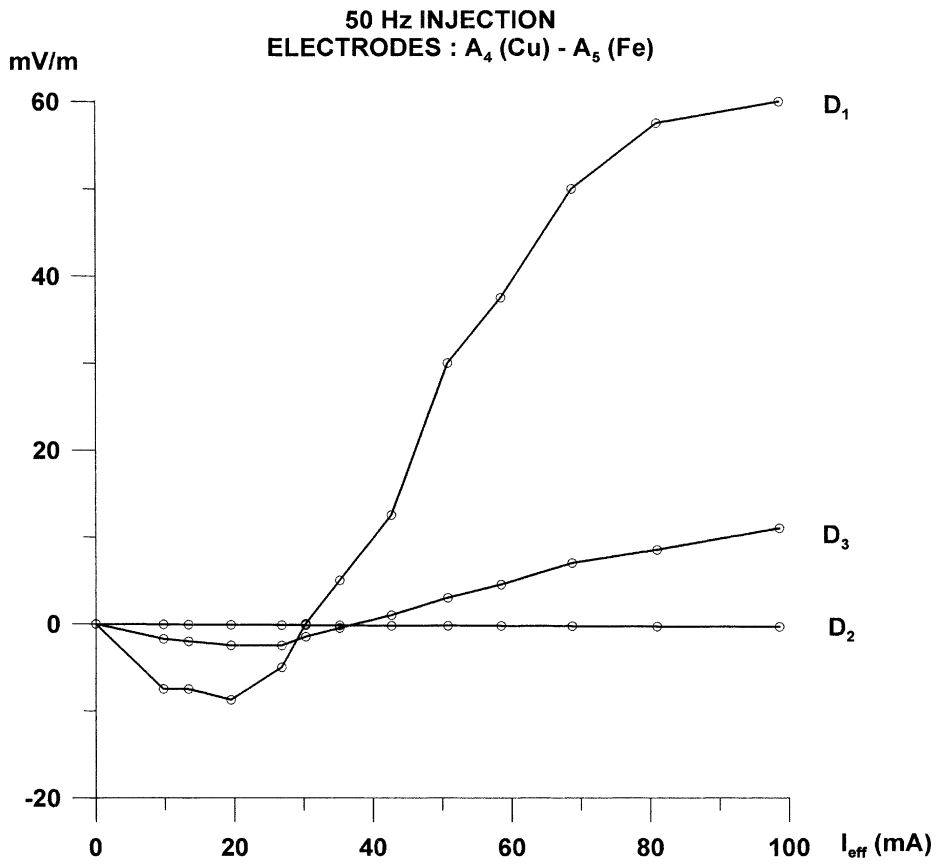

Fig. A10. The 50 Hz injection between A_4 and A_5. Variation of the amplitudes of the pulse signals vs. ac current intensity for the three dipoles D_1, D_2 and D_3.

in galvanic injection. This demonstrates that a metal–electrolyte interface and the corresponding redox couples are dramatically modified by the ac current flow.

To conclude, this study demonstrates that a dc voltage can be generated by a galvanic cell or an ac electrolytic cell. To our knowledge, it is the first time the relevance of this type of signals has been demonstrated in geophysical environments. These results shed some light on the origin of some noise signals observed in the ULF band, unexplained up to now. They can be generalized and extrapolated to various field scales.

References

Bard, A.J., Faulkner, L.R., 1980. Electrochemical Methods, Wiley, New York, 718 pp.

Besson, J., 1984. Précis de thermodynamique et cinétique électrochimiques. Edition Marketing, 446 pp.

Geller, R.J., 1996. VAN: a critical evaluation. In: Lighthill, J. (Ed.), A Critical Review of VAN. World Scientific, Singapore, pp. 155–238.

Papadopoulos, G.A., Drakatos, G., Papanastassiou, D., Kalogeras, I., Stavrakakis, G.N., 2000. Preliminary results about the catastrophic earthquake of 7 September 1999 in Athens. Greece Seism. Res. Lett. 71, 318–329.

Pavlides, S.B., Papadopoulos, G.A., Ganas, A., 1999. The 7th September, 1999 unexpected earthquake of Athens: preliminary results on the seismotectonic environment. In: Proceedings of the First Conference on the Advances on Natural Hazards Mitigation, Programme Reports, Athens, Greece, 3–4 November, pp. 80–85.

Pavlides, S.B., Papadopoulos, G.A., Ganas, A., 2000. Seismic hazard in urban areas: the 7th September 1999 Athens earthquake case study, In: Okumura, K., Takada, Goto, H. (Eds.), Proceedings of the Hokudan International Symposium and School on Active Faulting: Active Fault Research for the New Millennium, 17–26 January 2000, pp. 367–370.

Pham, V.N., Boyer, D., Therme, P., Yuan, X.C., Li, L., Jin, G.Y., 1986. Partial melting zones in the crust in Southern Tibet from magnetotelluric results. Nature 319, 310–314.

Pham, V.N., Boyer, D., Le Mouël, J.-L., Chouliaras, G., Stavrakakis, G.N., 1999. Electromagnetic signals generated in the solid earth by digital transmission of radio-waves as a plausible source for some so-called seismic electric signals. Phys. Earth Planet. Int. 114, 141–163.

Pham, V.N., Bernard, P., Boyer, D., Chouliaras, G., Le Mouël, J.-L., Stavrakakis, G.N., 2000. Electrical conductivity and crystal structure beneath the central Hellenides around the Gulf of Corinth (Greece) and their relationship with the seismotectonics. Geophys. J. Int. 142, 948–969.

Pham, V.N., Boyer, D., Perrier, F., Le Mouël, J.-L., 2001. Mécanismes de génération de bruits telluriques dans la bande ultrabasse fréquence (UBF): sources possibles des signaux dits signaux électro-sismiques (SES) (with abridged English version). C. R. Acad. Sci. Paris 333, 255–262.

Rochaix, C., 1996. Electrochimie: Thermodynamique-Cinétique, Nathan, Paris, 238 pp.

Stavrakakis, G.N., Drakatos, G., Papadopoulos, G.A., Papanastasiou, D., 1999. Characteristics of the aftershock sequence of the Athens earthquake of 7 September 1999, based on a local seismographic array. In: Proceedings of the Presention at the First Conference on the Advances on Natural Hazards Mitigation, Programme Abstracts, Athens, Greece, 3–4 November, 65 pp.

Tselentis, G.A., Zahradnik, J., 2000. Aftershock monitoring of the Athens earthquake of 7th September 1999. Seism. Res. Lett. 71, 330–337.

Uyeda, S., Nagao, T., Orihara, Y., Yamaguchi, T., Takahashi, I., 2000. Geoelectric potential changes: possible precursors to earthquake in Japan. PNAS 97, 4561–4566.

Varotsos, P., Alexopoulos, K., 1984. Physical properties of the variations of the electric field of the earth preceding earthquakes, I. Tectonophysics 110, 73–98.

Varotsos, P., Alexopoulos, K., Lazaridou, M., 1993. Latest aspects of earthquake prediction in Greece based on seismic electric signals, II. Tectonophysics 224, 1–37.

Varotsos, P., Lazaridou, M., Eftaxias, K., Antonopoulos, G., Makris, J., Kopanas, J., 1996a. Short-term earthquake prediction in Greece by seismic electric signals. In: Lighthill, J. (Ed.), A Critical Review of VAN, World Scientific, Singapore, pp. 29–76.

Varotsos, P., Eftaxias, K., Lazaridou, M., Nomicos, K., Sarlis, N., Bogris, N., Makris, J., Antonopoulos, G., Kopanas, J., 1996b. Recent earthquake prediction results in Greece based in the observation of seismic electric signals. Acta Geophys. Pol. 44, 301–327.

Varotsos, P., Eftaxias, K., Hadjicontis, V., Bogris, N., Skordas, E., Kapiris, P., Lazaridou, M., 1999a. A note on the extent of the SES sensitive area around Lamia (LAM). Greece Acta Geophys. Pol. 47, 436–439.

Varotsos, P., Eftaxias, K., Hadjicontis, V., Bogris, N., Skordas, E., Kapiris, P., Lazaridou, M., 1999b. A note on the extent of the SES sensitive area around Lamia (LAM). Greece Continuation. I. Acta Geophys. Pol. 47, 441–442.

Varotsos, P., Eftaxias, K., Hadjicontis, V., Bogris, N., Skordas, E., Kapiris, P., Lazaridou, M., 1999c. A note on the extent of the SES sensitive area around Lamia (LAM). Greece Continuation. II. Acta Geophys. Pol. 47, 443.